



OPEN Transmission dynamics and stability analysis of fractional HIV and AIDS epidemic model with antiretroviral therapy

Lili Huang¹, Yasir Nadeem Anjam², Akhtar Ali³✉, Basit Rehman³ & Muhammad Ateeq Tahir⁴

Worldwide populations have historically experienced serious issues from infectious diseases, requiring coordinated and inclusive prevention measures. HIV is one of the most hazardous of these as it attacks CD4⁺ cells, or T-cell lymphocytes, which are crucial to human immunity. To explore the variability of HIV/AIDS transmission, this study introduces a nonlinear stochastic mathematical model that incorporates a recovery compartment to account for hospitalized patients' progression to complete recovery and to better capture the intricate dynamics of disease transmission. Fractional derivatives are used with a generalized Caputo operator to enhance the accuracy of the model, effectively mixing the memory and genes that exist in biological systems. The model's validity is affirmed through considerations of positivity, boundedness, reproduction number, stability, and sensitivity analysis. Stability theory is employed to explore both local and global stabilities. Sensitivity analysis identifies parameters with a significant impact on the reproduction number. To establish the existence and uniqueness of solutions, the model is qualitatively examined via fixed-point theory. Apart from that, a new numerical technique for simulations focused on the predictor-corrector strategy is implemented and MATLAB is used to verify the results. By comparing the fractional-order and integer-order derivatives, it is noted that the fractional-order method is the more accurate and realistic depiction of the dynamics of the disease. The suggested technique unlocks the door for more effective interventions giving researchers a competitive edge in learning about and managing the complex mechanisms of HIV/AIDS transmission.

Keywords HIV-AIDS epidemic model, Existence and uniqueness, Generalized Caputo derivative, Adaptive P–C approach, Numerical simulation

HIV, the human immunodeficiency virus, progressively debilitates the immune system, eventually resulting in Acquired Immune Deficiency Syndrome (AIDS), where the immune system is significantly impaired. A condition triggered by a pathogen that assaults lymphocytes, ensuing in a lessened defense against contaminated aliment, is also referred to as HIV. The latter stage, dubbed AIDS, can take a patient anywhere from 2 to 15 years to manifest. AIDS can be marked by particular cancers, ailments, or other devastating clinical manifestations. It is generally thought that over 30 million people perished from HIV over the span of 30 years and that 7000 fresh instances of the virus are contracted abroad entire day. An estimated 44% of new pathogens in 2015 were thought to have emanated from substantial groups and their spouses. Around one-fourth of all fatalities annually are triggered by accessible aliment, leading to severe repercussions for civilization¹. According to HIV/AIDS data in 2021, over 38.4 million [33.9–43.8 million] individuals around the world are HIV positive, 1.5 million [1.1–2 million] individuals have been impacted with HIV, 650,000 [510,000–860,000] individuals expired from illness that associated with AIDS, and 28.7 million individuals are approaching antiretroviral therapy².

Screening CD4⁺ lymphocytes is a frequently utilized approach to monitoring the immune system's effectiveness. Various personal fluids, such as plasma, sperm, pre-coughing fluid, secretions from the genitals,

¹Department of Infectious Diseases, The Affiliated Yongchuan Hospital of Chongqing Medical University,, No. 439, Xuanhua Road, Yongchuan District, Chongqing 402160, China. ²Department of Applied Sciences, National Textile University, Faisalabad 37610, Pakistan. ³Department of Mathematics, Government College University, Faisalabad 38000, Pakistan. ⁴School of Digital Technologies, Narxoz University, Almaty, Kazakhstan. ✉email: utm.akhtar@gmail.com

and infant milk, are capable of enacting HIV from an HIV-positive individual to an AIDS-negative adult. HIV cannot momentarily be curable or averted, but it may be regulated with adequate medical assistance. ART diminishes the probability of conveying HIV, prolongs frequently destiny, and enhances well-being³. Drug resistance (DR) could hamper the therapeutic effect of ART agents, yet they have proven productive in lessening the prevalence of HIV as well as the associated mortality and morbidity. HIV-DR is marked by a mutation in the genetic code of HIV which renders it attainable to safely prevent the replication of the virus with a particular medication or a mixture of pharmaceuticals^{4,5}. A deep understanding of HIV transmission dynamics is crucial for developing operative prevention and treatment approaches. Mathematical modeling plays a vigorous role in examining viral epidemiology, evaluating interventions, predicting future trends, and addressing serious social challenges.

In recent years, fractional calculus has appeared as a dominant tool for modeling complex systems, allowing the calculation of derivatives and integrals of any positive real order. This ability has significantly improved models by integrating non-local physiognomies and memory effects⁶. Several fractional derivative methods, such as the Riemann–Liouville, Katugampola, Hadamard, and Caputo derivatives, have proved their efficacy in improving the precision of simulations for Real-life occurrences^{8,28}. The idea of fractional derivatives was initially introduced by Riemann–Liouville in 1832 and far ahead refined by Caputo in 1967. Caputo's devising comprised initial and boundary conditions, making it more pertinent for solving practical problems^{5,7,10}. Each derivative operator is intended to cater to precise system dynamics and present varying degrees of flexibility based on the requirements. Numerical, iterative methods and computational techniques have been widely applied to study fractional-order mathematical models^{9,29}.

Recent studies have progressive numerical approaches, for instance, the A–B Forth Moulton approach presented by Baleanu⁸, under the context of the generalized Caputo operator (GCO). Mathematical models are characteristically classified as either deterministic or stochastic. For example, Li et al.¹¹ estimated the dynamic behavior of models using both the SFD and NSFD methods. An ensemble-based approach with a temporal lag, reflecting the delay in a virus's ability to infect healthy T cells, was discovered by Roy et al.¹². Wu et al.⁸ examined the erratic conduct and permanency of fractional differential equations (FDEs) under a generalized Caputo derivative framework. Cai et al.¹³ examined a model that incorporated the phases of symptomatic and asymptomatic development for infected individuals, enabled by a variety of treatments. Goyal et al.¹⁴ evaluated disease dynamics using the fractal fractional derivative operators (FDOs) and the Caputo–Fabrizio. To study the spread of HIV/AIDS, Aslam et al.¹⁵ constructed an FDO with a Mittag–Leffler kernel. The concept of piecewise FDEs employing the Atangana–Baleanu derivative was introduced by Iqbal et al.¹⁶, and an integer-order nonlinear HIV/AIDS propagation model was constructed by Shaiful et al.¹⁷ as a modification of a non-integer model. Additional notable publications include Jan et al.¹⁸, who proposed a model explaining the dynamics of HIV/AIDS transmission between genders, and Naik et al.¹⁹, who evaluated novel HIV/AIDS models using Caputo fractional derivatives. Piqueira et al.²⁰ developed a model that brought social network effects into account. Kumar et al.²¹ evaluated an HIV transmission model using fractional-order approaches.

Anjam et al.²⁶ utilized fractal-fractional derivatives via the Caputo operator to investigate HIV transmission patterns across three infection levels. A TB–HIV co-infection model incorporating exogenous reinfection and recurrent TB was studied using a non-local operator with a Mittag–Leffler kernel²⁷. New models have been developed to study disease transmission, including a reaction–diffusion model for HIV/AIDS, emphasizing its chronic nature and socioeconomic impacts³⁴; a Chagas–HIV model with fractional operators³⁵; and a reaction–diffusion framework for SARS-CoV-2 to enhance public health strategies³⁷. Additionally, an Artificial Neural Network (ANN)-based framework was introduced to model Ebola transmission dynamics and long-term outcomes³⁸.

Further advancements include mathematical models for Monkeypox transmission in humans and rodents³⁹, Hepatitis B using fractional-order dynamics with memory effects⁴⁰, and malaria in Africa incorporating treatment and vaccination strategies via the Atangana–Baleanu fractional derivative⁴¹. The study also explores the complex joint dynamics of bovine tuberculosis (bTB) and rabies, highlighting the challenges posed by their differing transmission mechanisms⁴². The versatility of fractional calculus in dynamic modeling, particularly in epidemiology, demonstrates its potential to address complex scientific problems and advanced computational techniques.

Several studies also have explored the mathematical modeling of HIV/AIDS dynamics using real-world data. A temporal fractional HIV/AIDS model with fractal dimensions was developed to examine the influence of awareness on the transmission dynamics of HIV/AIDS in India, utilizing actual data from 1990 to 2016 to validate the proposed model³⁰. Similarly, Ref³², employed mathematical models to forecast the outbreaks of HIV/AIDS—one of the most critical public health challenges—in South Africa from 1990 to 2021, aiming to assess the country's preparedness for combating the epidemic in the near future. Furthermore, a mathematical model was formulated to investigate the dynamics of HIV/AIDS in real-world scenarios, incorporating reported HIV/AIDS statistics from Pakistan (1992–2020) to analyze its transmission patterns and conduct a comprehensive mathematical assessment³³.

In order to accurately model the long-term dynamics, crossover behavior, and memory effects of HIV transmission, it is necessary to choose the proper fractional operator and kernel type. The Caputo operator is an important decision in this situation because of its power-law kernel, which is exceptionally equipped for preserving these memory effects and long-term interactions. These features serve as vital for accurately modeling the intricate dynamics of HIV transmission because they enable a realistic depiction of the various elements that contribute to the virus's spread. These components include individual behavior, social attitudes, healthcare restrictions, and the efficacy of treatments, each of which is important for analyzing and preventing HIV spread. As a result of this awareness, the study has shifted its attention to the findings' deeper implications.

This research investigates the dynamics of HIV transmission by establishing a compartment for recovered persons, which accounts for the implementation of hospitalized patients to recovery. The model is dependent on a generalized Caputo fractional operator (CFO) with two fractional-order variables, considerably improving its potential to capture genetic and memory effects. Six different compartments are used to classify the population. The model's dependability is verified by a thorough study that uses the fixed-point theory framework to verify the existence and uniqueness of solutions. The significance of the research is tackled by establishing a new numerical method for simulations based on the predictor–corrector approach, which is validated in MATLAB. Simulation results are graphically presented for various fractional orders, allowing for comparisons with integer-order models. This study underscores the efficacy of the fractional approach, highlighting the model's sensitivity to changes in fractional orders.

The subsequent sections of the article are ordered as follows: “Essential preliminaries” offers a brief explanation of fractional-order calculus, whereas “Model construction” defines the model formulation and its fractional representation. “Qualitative analysis of model” concentrates on model analysis, and sensitivity analysis, and also discusses the stability aspects of the model under consideration. “Theoretical exploration of the FO HIV dynamics” provides the validation of the existence and uniqueness of the solution. “Numerical techniques for the devised model” offers specifics of the numerical simulations by using the novel predictor-corrector-based numerical technique and application to the proposed model. The numerical solutions are presented in “Results and discussion”, whereas the discussion of results is given. Finally, “Conclusion” offers a concise summary of the article.

Essential preliminaries

In this segment, the main definitions of generalized fractional operators from earlier research are reviewed, which will be applied in the study^{22–24}.

Definition The generalized fractional integral of a function $z(\hat{p})$, is specified as $\delta \in (k - 1, k]$, while $k \in N$ (if remains integral)

$$I_{a+}^{\delta, \sigma} z(\hat{p}) = \frac{\sigma^{(1-\delta)}}{\Gamma(\delta)} \int_a^{\hat{p}} \xi^{(\sigma-1)} (\hat{p} - \xi^\sigma)^{\delta-1} z(\xi) d\xi, \hat{p} > a, \quad (1)$$

where $\sigma > 0$, and $a \geq 0$.

Definition The parameter order δ of generalized Caputo derivative (GCD) for $z(\hat{p})$ is specified that $\delta \in (k - 1, k]$, while $k \in N$ and $\sigma > 0$, $a \geq 0$, then

$${}^C D_{a+}^{\delta, \sigma} z(\hat{p}) = I_{a+}^{k-\delta, \sigma} (X^k z)(\hat{p}) = \frac{\sigma^{(\delta-k+1)}}{\Gamma(k-\delta)} \int_a^{\hat{p}} \xi^{(\sigma-1)} (\hat{p} - \xi^\sigma)^{k-\delta-1} X^k z(\xi) d\xi, \hat{p} > a, \quad (2)$$

where $X = (\xi^{(1-\sigma)} \frac{d}{d\xi})$, and approach the new derivative as an isolated case, when $\delta \in (0, 1)$ and $a = 0$, the new form GCD is given as follows:

$${}^C D_{a+}^{\delta, \sigma} z(\hat{p}) = \frac{\sigma^{(\delta)}}{\Gamma(1-\delta)} \int_0^{\hat{p}} (\hat{p} - \xi^\sigma)^{-\delta} z'(\xi) d\xi, \hat{p} > 0. \quad (3)$$

Model construction

Analyzing the dynamics of HIV transmission and establishing effective preventative and treatment strategies are both enhanced by the incorporation of mathematical models. It is essential to construct such models using epidemiological strategies in order to provide insight into the basic mechanisms of HIV transmission. It is essential to determine important factors to mitigate HIV transmission. The development of prevention and treatment strategies has benefited tremendously from the construction and documentation of several HIV transmission models that depend on infectious mechanisms.

This research is centered on investigating the dynamics of HIV-AIDS transmission by presenting a compartment for recovered individuals, which accounts for the transition of hospitalized patients to recovery. The model construction distributes the whole populace of humanity into six distinct subsets those are outlined beneath: Susceptible uninformed populace (\tilde{S}_u), the Susceptible informed populace (\tilde{S}_i), the HIV-infected populace (\tilde{I}), the AIDS-afflicted people (\tilde{A}), the HIV-infected populace with ART medication (\tilde{C}), and the recovered individuals (\tilde{R}). Entirely population is indicated by \tilde{E}_p that is specified as:

$$\tilde{E}_p = \tilde{S}_u + \tilde{S}_i + \tilde{I} + \tilde{A} + \tilde{C} + \tilde{R}.$$

The rate at which susceptible individuals acquire the infection through interacting with infectious individuals is the force of infection in our model. It depicts the dynamics of disease transmission by quantifying the risk of infection per capita and capturing the interplay between susceptible and infected populations.

Moreover, the assumptions employed in formulating the mathematical model for the spread of HIV/AIDS are as follows:

- The individuals \tilde{C} and \tilde{A} are assumed not to spread HIV due to their specific condition.
- The population \tilde{A} is assumed not to spread HIV, as the AIDS population is considered too ill to transmit the virus (until isolated).
- Unaware individuals \tilde{S}_u can transition to becoming aware \tilde{S}_i , but the reverse is not possible.
- Individuals with AIDS who begin antiretroviral therapy (ART) will transition into the treated population and will remain in this group if they consistently adhere to the therapy.
- It is supposed that individuals suffering from HIV and AIDS have access to antiretroviral therapy (ART) treatment.
- The mortality rate due to HIV/AIDS is assumed to occur only among individuals affected by AIDS.

Based on the aforementioned principles, Fig. 1 illustrates the flow pattern of interaction between the different stages of infectious diseases. Thus, the integer-order model with a consciousness alter regarding HIV-AIDS propagation is specified as:

$$S'_u = X - \frac{\tilde{S}_u \tilde{I} \gamma_1}{\tilde{E}_p} - \tilde{S}_u (\omega_{(1)}^* + \rho_1),$$

$$S'_i = \tilde{S}_u \rho_1 - \frac{\tilde{S}_i \tilde{I} \gamma_1}{\tilde{E}_p} (1 - \xi_1) - \tilde{S}_i \omega_{(1)}^*,$$

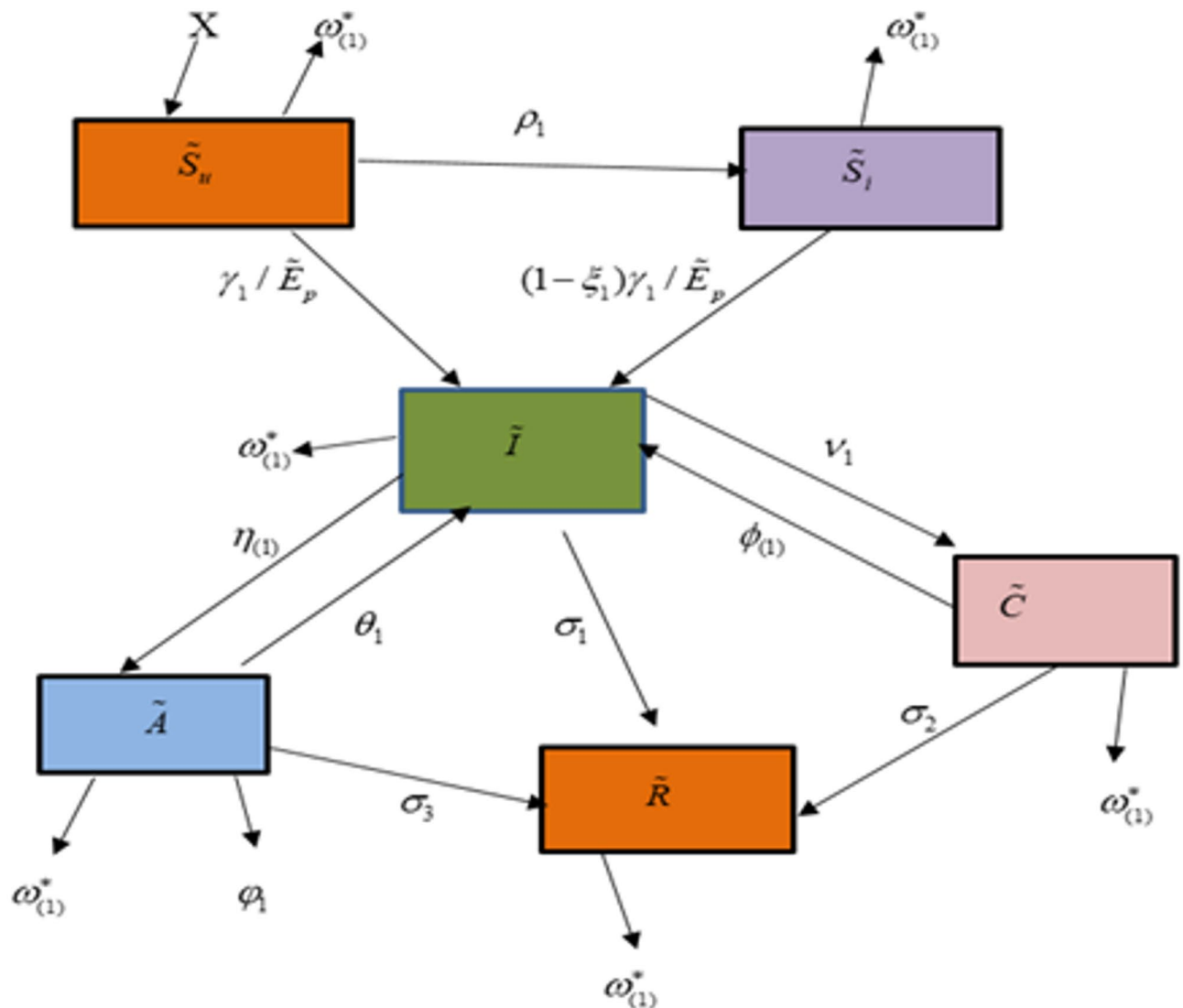


Fig. 1. Schematic flow of the proposed model.

$$\begin{aligned}
 I' &= (\tilde{S}_i(1 - \xi_1) + \tilde{S}_u) \frac{\tilde{I}\gamma_1}{\tilde{E}_p} + \tilde{C}\phi_{(1)} + \tilde{A}\theta_1 - \tilde{I}(\omega_{(1)}^* + \nu_1 + \eta_{(1)}), \\
 A' &= \tilde{I}\eta_{(1)} - \tilde{A}(\varphi_1 + \omega_{(1)}^* + \theta_1), \\
 C' &= \tilde{I}\nu_1 - \tilde{C}(\omega_{(1)}^* + \phi_{(1)}), \\
 R' &= \tilde{I}\sigma_1 + \tilde{C}\sigma_2 + \tilde{A}\sigma_3 - \tilde{R}\omega_{(1)}^*
 \end{aligned}
 \tag{4}$$

Hence, the initial conditions are:

$$\tilde{S}_u(0) = E_1, \tilde{S}_i(0) = E_2, \tilde{I}(0) = E_3, \tilde{C}(0) = E_4, \tilde{A}(0) = E_5, \tilde{R}(0) = E_6.$$

This model (4) is constructed here using the newly introduced GCFD. The following is the appraised rendition of the proposed model:

$$\begin{aligned}
 {}^C D_0^{\delta, \sigma} \tilde{S}_u &= X - \frac{\tilde{S}_u \tilde{I} \gamma_1}{\tilde{E}_p} - \tilde{S}_u(\omega_{(1)}^* + \rho_1), \\
 {}^C D_0^{\delta, \sigma} \tilde{S}_i &= \tilde{S}_u \rho_1 - \frac{\tilde{S}_i \tilde{I} \gamma_1}{\tilde{E}_p} (1 - \xi_1) - \tilde{S}_i \omega_{(1)}^*, \\
 {}^C D_0^{\delta, \sigma} \tilde{I} &= (\tilde{S}_i(1 - \xi_1) + \tilde{S}_u) \frac{\tilde{I} \gamma_1}{\tilde{E}_p} + \tilde{C}\phi_{(1)} + \tilde{A}\theta_1 - \tilde{I}(\omega_{(1)}^* + \nu_1 + \eta_{(1)}), \\
 {}^C D_0^{\delta, \sigma} \tilde{A} &= \tilde{I}\eta_{(1)} - \tilde{A}(\varphi_1 + \omega_{(1)}^* + \theta_1), \\
 {}^C D_0^{\delta, \sigma} \tilde{C} &= \tilde{I}\nu_1 - \tilde{C}(\omega_{(1)}^* + \phi_{(1)}), \\
 {}^C D_0^{\delta, \sigma} \tilde{R} &= \tilde{I}\sigma_1 + \tilde{C}\sigma_2 + \tilde{A}\sigma_3 - \tilde{R}\omega_{(1)}^*,
 \end{aligned}
 \tag{5}$$

where the following is an outline of the model parameters mentioned above:

- X indicates the susceptible uninformed,
- γ_1 For the HIV acquisition rate,
- ρ_1 symbolizes the rapid rate at which S_u changes into S_i ,
- $\omega_{(1)}^*$ signifies the frequency of natural mortality,
- $\phi_{(1)}$ shows the number of people in class C who go to class I.
- θ_1 symbolizes the clip at which A shifts to I.
- ν_1 illustrates the rate of improvement in class I subsequent toward class C.
- $\eta_{(1)}$ depicts rapidity while A converts from I.
- φ_1 reflects the mortality rate from AIDS.
- $\sigma_1, \sigma_2, \sigma_3$ identify the extent of recurrence from infected people S_u to S_i and from hospitalized patients to recovered cases.
- ξ_1 Indicates the proportion of S_i those who get an infection.

Qualitative analysis of model

In the upcoming section, our study will emphasize the mathematical formulation encapsulated in the model (4). Our investigation will delve into the aspects of boundedness and positivity within the model. Additionally, we will determine the equilibrium points and compute the basic reproduction number. The sensitivity analysis and the local stability and global stability of the developed model at equilibrium points are also explored.

Positivity

Positivity constraints are imposed on both the initial conditions and parameters in the devised model, ensuring that their values remain non-negative or greater than zero throughout the modeling process. This imposition enhances the model's reliability by minimizing the occurrence of unrealistic outcomes, thereby improving its applicability and making it more representative of real-world scenarios and behaviors.

Theorem 4.1 We assume a positive initial value for the problem specified in Eq. (4) and if the solutions to the model in Eq. (4) exist, they will be positive for all time $t > 0$.

Proof Let us consider the first equation of the devised model (4) as

$$\frac{d\tilde{S}_u}{dt} = X - \frac{\tilde{S}_u \tilde{I} \gamma_1}{\tilde{E}_p} - \tilde{S}_u (\omega_{(1)}^* + \rho_1).$$

By constant formula of alternation provides the solution

$$\begin{aligned}\tilde{S}_u(t) = \tilde{S}_u(0) \exp \left[- \int_0^t (\omega_1^* + \rho_1) dt - \omega_1^* t \right] + \exp \left[- \int_0^t (\omega_1^* + \rho_1) dt - \omega_1^* t \right] X \\ \left(X - \frac{\tilde{S}_u \tilde{I} r_1}{\tilde{E}_p} \right) \int \exp \left[\int_0^t (\omega_1^* + \rho_1) dt - \omega_1^* t \right] dt.\end{aligned}$$

Hence, $\tilde{S}_u(t) \geq 0$ for all time $t > 0$.

Similarly, it can be shown that $\tilde{S}_i \geq 0, \tilde{I} \geq 0, \tilde{A} \geq 0, \tilde{C} \geq 0, \tilde{R} \geq 0$.

Invariant region

We determined the invariant region where the solution of the proposed model is bounded. Now, consider the total population of the given model as:

$$\tilde{E}_p = \tilde{S}_u + \tilde{S}_i + \tilde{I} + \tilde{A} + \tilde{C} + \tilde{R}. \quad (6)$$

Now, differentiate Eq. (6) provides

$$\frac{d\tilde{E}_p}{dt} = \frac{d\tilde{S}_u}{dt} + \frac{d\tilde{S}_i}{dt} + \frac{d\tilde{I}}{dt} + \frac{d\tilde{A}}{dt} + \frac{d\tilde{C}}{dt} + \frac{d\tilde{R}}{dt}. \quad (7)$$

Substituting all the state equations from the model (4) into Eq. (7) yields

$$\frac{d\tilde{E}_p}{dt} = X - \omega_1^* \tilde{E}_p. \quad (8)$$

Taking integration on both sides of Eq. (8) with $t \rightarrow \infty$, one obtains $\tilde{E}_p \leq \frac{X}{\omega_1^*}$.

Thus, $\tilde{E}_p(t) \leq \frac{X}{\omega_1^*}$ as $t \rightarrow \infty$

$$\Omega = \left\{ \tilde{S}_u, \tilde{S}_i, \tilde{I}, \tilde{A}, \tilde{C}, \tilde{R} \in R_+^6 : \tilde{S}_u + \tilde{S}_i + \tilde{I} + \tilde{A} + \tilde{C} + \tilde{R} \leq \frac{X}{\omega_1^*} \right\}.$$

Clearly, Ω is positively invariant.

Equilibrium points

Equilibrium points indicate in stable condition in the progression of the disease, where the occurrence of new infections is offset by combined occurrences of recoveries and deaths. Equilibrium points have two important types disease-free and endemic equilibrium. Disease Free Equilibrium (DFE) represents when there is no disease in the population. To calculate DFE D_0 , we put $\frac{d\tilde{I}}{dt}, \frac{d\tilde{A}}{dt}, \frac{d\tilde{C}}{dt}, \frac{d\tilde{R}}{dt} = 0$. Expect the susceptible class \tilde{S}_u, \tilde{S}_i , which we set to its initial values.

This point helps us to compare disease behavior in the presence and absence of disease.

$$D_0 = \left(\tilde{S}_u(0), \tilde{S}_i(0), 0, 0, 0, 0 \right),$$

$$D_0 = \left(\frac{X}{\omega_1^* + \rho_1}, \frac{\tilde{S}_u \rho_1}{\omega_1^*}, 0, 0, 0, 0 \right)$$

Now, the endemic equilibrium points are calculated as:

$$D^* = \left(\tilde{S}_u^*, \tilde{S}_i^*, \tilde{I}^*, \tilde{A}^*, \tilde{C}^*, \tilde{R}^* \right),$$

where,

$$\tilde{S}_u^* = \frac{X \tilde{E}_p}{\tilde{I} r_1 + (\omega_1^* + \rho_1)},$$

$$\begin{aligned}\tilde{S}_i^* &= \frac{X \tilde{E}_p \rho_1}{\left[\tilde{I} r_1 + (\omega_1^* + \rho_1) \right] \left[\tilde{I} r_1 (1 - \xi_1) - \omega_1^* \tilde{E}_p \right]}, \\ \tilde{I}^* &= \frac{\tilde{E}_p (\omega_1^* + \varphi_1) (\varphi_1 + \omega_1^* + \theta_1) (\omega_1^* + \nu_1 + \eta_1) - \left(\tilde{S}_i^* (1 - \xi_1) + \tilde{S}_u^* \right) r_1 + \nu_1 + \eta_1}{\left(\tilde{S}_i^* (1 - \xi_1) + \tilde{S}_u^* \right) r_1 + \nu_1 + \eta_1}, \\ \tilde{A}^* &= \frac{\tilde{I} \eta_1}{(\varphi_1 + \omega_1^* + \theta_1)}, \\ \tilde{C}^* &= \frac{\tilde{I} \nu_1}{\omega_1^* + \varphi_1}, \\ \tilde{R}^* &= \frac{[\sigma_1 (\varphi_1 + \omega_1^* + \theta_1) + \nu_1 \theta_1 + \eta_1] \tilde{I}}{\omega_1^* (\varphi_1 + \omega_1^* + \theta_1)}.\end{aligned}$$

The basic reproduction number

The threshold value, or basic reproduction number R_0 , is a widely employed statistic for evaluating a communicable disease's transmissibility or contagiousness. In a vulnerable group, it represents the average amount of people infected by a single infectious person. Biologically, it reflects the contagiousness and transmissibility of a pathogen. If $R_0 > 1$, it indicates that the disease has the potential to sustain transmission within the population, leading to an outbreak. Conversely, if $R_0 < 1$, the infection is unlikely to establish a self-sustaining chain of transmission, and it may eventually die out in the population. Using the principle of the next-generation matrix, it is calculated as

$$F = \begin{bmatrix} \frac{\left(\tilde{S}_i (1 - \xi_1) + \tilde{S}_u \right) r_1}{\tilde{E}_p} & 0 & 0 \\ 0 & 0 & 0 \\ 0 & 0 & 0 \end{bmatrix}.$$

$$V = \begin{bmatrix} (\omega_1^* + \nu_1 + \eta_1) & 0 & 0 \\ 0 & (\varphi_1 + \omega_1^* + \theta_1) & 0 \\ 0 & 0 & c (\omega_1^* + \varphi_1) \end{bmatrix}.$$

Therefore, the reproduction number R_0 for our devised model (5) is the spectral radius of the next generation matrix FV^{-1} and calculated as,

$$FV^{-1} = \begin{bmatrix} \frac{\left(\tilde{S}_i (1 - \xi_1) + \tilde{S}_u \right) r_1}{\tilde{E}_p (\omega_1^* + \nu_1 + \eta_1)} & 0 & 0 \\ 0 & 0 & 0 \\ 0 & 0 & 0 \end{bmatrix}. \quad (9)$$

Therefore, from Eq. (9), the reproduction number R_0 is calculated as:

$$R_0 = \frac{\left(\tilde{S}_i (1 - \xi_1) + \tilde{S}_u \right) r_1}{\tilde{E}_p (\omega_1^* + \nu_1 + \eta_1)}.$$

Now, by putting initial values yields

$$R_0 = \frac{(E_2 (1 - \xi_1) + E_1) y_1}{\tilde{E}_p (\omega_1^* + \nu_1 + \eta_1)}.$$

Sensitivity analysis

The degree of influence of input parameters over the dynamics of infectious model is assets through the launch of sensitivity analysis. The sensitivity indices of the infectious disease model given in (4) are deduced by using the approach of Chitnis. Now, the normalized forward sensitivity indices of a parameter x of R_0 is calculated as

$$\Delta_x^{R_0} = \frac{\partial R_0}{\partial x} \frac{x}{R_0}.$$

The estimated sensitivity projected in reproduction number with respect to various parameters is given as

$$\begin{aligned}\Delta_{y_1}^{R_0} &= \frac{\partial R_0}{\partial y_1} \cdot \frac{y_1}{R_0} = 1, \\ \Delta_{\omega_1^*}^{R_0} &= \frac{\partial R_0}{\partial \omega_1^*} \cdot \frac{\omega_1^*}{R_0} = -0.0729, \\ \Delta_{v_1}^{R_0} &= \frac{\partial R_0}{\partial v_1} \cdot \frac{v_1}{R_0} = 0.0017956, \\ \Delta_{\xi_1}^{R_0} &= \frac{\partial R_0}{\partial \xi_1} \cdot \frac{\xi_1}{R_0} = -0.165, \\ \Delta_{\eta_1}^{R_0} &= \frac{\partial R_0}{\partial \eta_1} \cdot \frac{\eta_1}{R_0} = 0.5585.\end{aligned}$$

Table 1 comprehends the directional projection of the parameters involved in the considered model explaining the viral infectious disease transmission flow. This analysis also shows the significance of various factors in the transmission of disease. The sensitivity indices indicate the set of parameters $S_1 = \{y_1, \nu_1, \eta_1\}$ and R_0 have a direct relationship and the set of parameters $S_2 = \{\omega_1^*, \xi_1\}$ has an inverse relationship with R_0 . This illustrates that the greater the value of the parameters S_1 greatly maximize the threshold value R_0 , but R_0 decreases by a greater value of S_2 .

The existence of a positive relationship is voted through the plus sign whereas the negative sign acknowledges the showing of the negative relationship between the parameters and the transmission rate.

Stability analysis

The system’s local and global stability are studied in this section. The eigenvalues of the Jacobian matrix at the equilibrium point are evaluated in order to ascertain local stability. The equilibrium is locally stable when all of the eigenvalues have negative real parts. On the other hand, global stability requires analyzing the behavior of the system across the entire domain, which frequently calls for advanced mathematical methods like Lyapunov analysis.

Local stability

The purpose of local stability analysis is to determine whether a small perturbation in the disease system will lead to disease persistence or eradication. Understanding local stability at equilibrium points is crucial in epidemiological modeling, as it provides insights into disease transmission dynamics and population-level spread. To demonstrate the local asymptotic stability of both the endemic equilibrium and disease-free equilibrium, the following theorems are presented.

Theorem 4.2 *The disease-free equilibrium D_0 is locally asymptotically stable when $R_0 < 1$, however, when $R_0 > 1$, it is unstable.*

Proof The Jacobin matrix of disease-free equilibrium point for the proposed model is given as

Parameter	Sensitivity indices
y_1	+
ω_1^*	−
ν_1	+
ξ_1	−
η_1	+

Table 1. Sensitivity indices and parameters of the reproduction number R_0

$$J(F_0) = \begin{bmatrix} -(\omega_1^* + \rho_1) - \frac{\tilde{I}r_1}{\tilde{E}_p} & 0 & & & \\ \rho_1 & -\frac{\tilde{I}r_1}{\tilde{E}_p}(1 - \xi_1) - \omega_1^* & & & \\ \frac{\tilde{I}r_1}{\tilde{E}_p} & \frac{(1 - \xi_1)\tilde{I}r_1}{\tilde{E}_p} & & & \\ 0 & 0 & & & \\ 0 & 0 & & & \\ 0 & 0 & & & \\ \left(\tilde{S}_i(1 - \xi_1) + \tilde{S}_u\right)\frac{r_1}{\tilde{E}_p} - (\omega_1^* + \nu_1 + \eta_1) & \theta_1 & \varphi_1 & & \\ \eta_1 & \theta_1 & 0 & & \\ \nu_1 & 0 & -(\omega_1^* + \varphi_1) & & \end{bmatrix}$$

The evaluation of the Jacobin at disease-free equilibrium provides

$$J(F_0) = \begin{bmatrix} -(\omega_1^* + \rho_1) & 0 & 0 & 0 & 0 \\ \rho_1 & -\omega_1^* & 0 & 0 & 0 \\ 0 & 0 & \left(\tilde{S}_i(1 - \xi_1) + \tilde{S}_u\right)\frac{r_1}{\tilde{E}_p} - (\omega_1^* + \nu_1 + \eta_1) & \theta_1 & \varphi_1 \\ 0 & 0 & \eta_1 & -(\varphi_1 + \omega_1^* + \theta_1) & 0 \\ 0 & 0 & \nu_1 & 0 & -(\omega_1^* + \varphi_1) \end{bmatrix}.$$

$$|J(F_0) - \lambda I| = \begin{bmatrix} -(\omega_1^* + \rho_1) - \lambda & 0 & 0 & 0 & 0 \\ \rho_1 & -\omega_1^* - \lambda & 0 & 0 & 0 \\ 0 & 0 & \left(\tilde{S}_i(1 - \xi_1) + \tilde{S}_u\right)\frac{r_1}{\tilde{E}_p} - (\omega_1^* + \nu_1 + \eta_1) - \lambda & \theta_1 & \varphi_1 \\ 0 & 0 & \eta_1 & -(\varphi_1 + \omega_1^* + \theta_1) - \lambda & 0 \\ 0 & 0 & \nu_1 & 0 & -(\omega_1^* + \varphi_1) - \lambda \end{bmatrix}.$$

By using the Routh–Hurwitz Criterion, it is verified that each eigenvalue of the polynomial equation contains a non-positive real part when $R_0 < 1$. As a result, the DFE point D_0 is locally asymptotically stable.

Theorem 4.3 *The endemic equilibrium point D^* will be locally asymptotically stable if the value $R_0 > 1$, however, when $R_0 < 1$, it is unstable.*

Proof

$$J(F^*) = \begin{bmatrix} -(\omega_1^* + \rho_1) - \frac{\tilde{I}r_1}{\tilde{E}_p} & 0 & 0 & 0 & 0 \\ \rho_1 & -\frac{\tilde{I}r_1}{\tilde{E}_p}(1 - \xi_1) - \omega_1^* & 0 & 0 & 0 \\ \frac{\tilde{I}r_1}{\tilde{E}_p} & \frac{(1 - \xi_1)\tilde{I}r_1}{\tilde{E}_p} & \left(\tilde{S}_i(1 - \xi_1) + \tilde{S}_u\right)\frac{r_1}{\tilde{E}_p} - (\omega_1^* + \nu_1 + \eta_1) & \theta_1 & \varphi_1 \\ 0 & 0 & \eta_1 & -(\varphi_1 + \omega_1^* + \theta_1) & 0 \\ 0 & 0 & \nu_1 & 0 & -(\omega_1^* + \varphi_1) \end{bmatrix}.$$

$$J(F^*) = \begin{bmatrix} -\mu_1 & 0 & 0 & 0 & 0 \\ \rho_1 & -\mu_2 & 0 & 0 & 0 \\ \frac{\tilde{I}r_1}{\tilde{E}_p} & \frac{(1 - \xi_1)\tilde{I}r_1}{\tilde{E}_p} & -\mu_3 & 0 & 0 \\ 0 & 0 & \eta_1 & -\mu_4 & 0 \\ 0 & 0 & \nu_1 & 0 & -\mu_5 \end{bmatrix}.$$

$$\text{where } \mu_1 = (\omega_1^* + \rho_1) - \frac{\tilde{I}r_1}{\tilde{E}_p}, \quad \mu_2 = \frac{\tilde{I}r_1}{\tilde{E}_p} (1 - \xi_1) - \omega_1^*,$$

$$\mu_3 = \left(\tilde{S}_i (1 - \xi_1) + \tilde{S}_u \right) \frac{r_1}{\tilde{E}_p} - (\omega_1^* + \nu_1 + \eta_1), \quad \mu_4 = (\varphi_1 + \omega_1^* + \theta_1), \quad \mu_5 = (\omega_1^* + \varphi_1).$$

It is clear that all eigenvalues of $J(F^*)$ have negative and real if $R_0 > 1$.

Global stability

Global stability analysis in a disease model determines whether the system converges to a stable equilibrium across all possible initial conditions. This analysis is crucial for understanding long-term disease dynamics and overall infection prevalence within a population. The following theorem establishes the conditions for globally asymptotically stable endemic and disease-free equilibrium points.

Theorem 4.4 *The disease-free equilibrium point F_0 is globally asymptotically stable for $R_0 < 1$, otherwise, unstable for $R_0 > 1$.*

Proof The subsequent Lyapunov function is precise and satisfies the settings of being positive definite with a negative definite derivative. To establish this result, we first present the Lyapunov function defined as:

$$\mathcal{L} = y_1 \tilde{S}_u + y_2 \tilde{S}_i + y_3 \tilde{I} + y_4 \tilde{A} + y_5 \tilde{C}. \quad (10)$$

where y_1, y_2, y_3, y_4, y_5 are constants. Now, by differentiating Eq. (10), one obtains

$$\mathcal{L}' = y_1 \tilde{S}_u' + y_2 \tilde{S}_i' + y_3 \tilde{I}' + y_4 \tilde{A}' + y_5 \tilde{C}'.$$

Putting the values from the model and arranging them provides

$$\begin{aligned} \mathcal{L}' = & \left\{ y_1 X - y_1 \frac{\tilde{I}r_1}{\tilde{E}_p} - y_1 (\omega_1^* + \rho_1) + y_2 \rho_1 + y_3 \frac{\tilde{I}r_1}{\tilde{E}_p} \right\} (\tilde{S}_u - \tilde{S}_u^\circ) \\ & + \left\{ y_3 (1 - \xi_1) \frac{\tilde{I}r_1}{\tilde{E}_p} - y_2 \frac{\tilde{I}r_1}{\tilde{E}_p} (1 - \xi_1) - y_2 \omega_1^* \right\} (\tilde{S}_i - \tilde{S}_i^\circ) \\ & + \{ y_4 \eta_1 - y_3 (\omega_1^* + \nu_1 + \eta_1) \} \tilde{I} + \{ y_3 \theta_1 - y_4 (\varphi_1 + \omega_1^* + \theta_1) \} \tilde{A} \\ & + \{ y_3 \varphi_1 + y_5 (\omega_1^* + \varphi_1) \} \tilde{C}. \end{aligned}$$

where $D_0 = \left(\frac{X}{\omega_1^* + \rho_1}, \frac{\tilde{S}_u \rho_1}{\omega_1^*} \right)$. It is observed that $\mathcal{L}'(t) \leq 0$ when $\tilde{S}_u > \tilde{S}_u^\circ$ and $\tilde{S}_i > \tilde{S}_i^\circ$ and $R_0 < 1$ and $\mathcal{L}' = 0$ if and only if $\tilde{S}_u = \tilde{S}_u^\circ, \tilde{S}_i = \tilde{S}_i^\circ$.

The Lasalle's invariance principle and $\tilde{I} = \tilde{A} = \tilde{C} = 0$. The Lyapunov function is positive definite, its derivative is negative definite and all of the conditions for the Lyapunov function are positive definite. Consequently, the DFE is globally asymptotically stable.

Theorem 4.5 *The endemic equilibrium point D^* is globally asymptotically stable if the value $R_0 > 1$, however, when $R_0 < 1$, it is unstable.*

Proof To prove the global stability of the proposed model at the endemic equilibrium point D^* , the Castillo Chevez method is used. Further, we consider the model as

$$\left. \begin{aligned} \frac{d\tilde{S}_u}{dt} &= X - \tilde{S}_u \frac{\tilde{I}r_1}{\tilde{E}_p} - \tilde{S}_u (\omega_1^* + \rho_1), \\ \frac{d\tilde{S}_i}{dt} &= \tilde{S}_i \rho_1 - \tilde{S}_i \frac{\tilde{I}r_1}{\tilde{E}_p} (1 - \xi_1) - \tilde{S}_i \omega_1^*, \\ \frac{d\tilde{I}}{dt} &= \left(\tilde{S}_i (1 - \xi_1) + \tilde{S}_u \right) \frac{\tilde{I}r_1}{\tilde{E}_p} + \tilde{C} \varphi_1 + \tilde{A} \theta_1 - \tilde{I} (\omega_1^* + \nu_1 + \eta_1). \end{aligned} \right\} \quad (11)$$

Taking the Jacobin and the additive compound matrix of order 2 for the Eq. (4.6), the following matrix is obtained

$$J = \begin{bmatrix} -a_{11} & 0 & 0 \\ a_{21} & -a_{22} & 0 \\ a_{31} & a_{32} & -a_{33} \end{bmatrix},$$

$$J^{[2]} = \begin{bmatrix} -(a_{11} + a_{22}) & a_{23} & -a_{13} \\ a_{32} & -(a_{11} + a_{22}) & a_{12} \\ -a_{31} & a_{21} & -(a_{22} + a_{33}) \end{bmatrix}, \quad (12)$$

Let $Q(x) = (\tilde{S}_u, \tilde{S}_i, \tilde{I}) = \text{diag} \left\{ \frac{\tilde{S}_u}{\tilde{S}_i}, \frac{\tilde{S}_u}{\tilde{S}_i}, \frac{\tilde{S}_u}{\tilde{S}_i} \right\}$ and then $Q^{-1}(x) = \text{diag} \left\{ \frac{\tilde{S}_i}{\tilde{S}_u}, \frac{\tilde{S}_i}{\tilde{S}_u}, \frac{\tilde{S}_i}{\tilde{S}_u} \right\}$, then the time derivative of the function $Q_f(x)$, suggests that

$$Q_f(x) = \text{diag} \left\{ \frac{\dot{\tilde{S}}_u}{\tilde{S}_i} - \frac{\tilde{S}_u \dot{\tilde{S}}_i}{\tilde{S}_i^2}, \frac{\dot{\tilde{S}}_u}{\tilde{S}_i} - \frac{\tilde{S}_u \dot{\tilde{S}}_i}{\tilde{S}_i^2}, \frac{\dot{\tilde{S}}_u}{\tilde{S}_i} - \frac{\tilde{S}_u \dot{\tilde{S}}_i}{\tilde{S}_i^2} \right\}. \quad (13)$$

Now, $Q_f Q^{-1} = \text{diag} \left\{ \frac{\dot{\tilde{S}}_u}{\tilde{S}_u} - \frac{\dot{\tilde{S}}_i}{\tilde{S}_i}, \frac{\dot{\tilde{S}}_u}{\tilde{S}_u} - \frac{\dot{\tilde{S}}_i}{\tilde{S}_i}, \frac{\dot{\tilde{S}}_u}{\tilde{S}_u} - \frac{\dot{\tilde{S}}_i}{\tilde{S}_i} \right\}$
And $QJ_2^{[2]}Q^{-1} = J_2^{[2]}.A = Q_f Q^{-1} + QJ_2^{[2]}Q^{-1}$, which can be described as

$$A = \begin{bmatrix} A_{11} & A_{12} \\ A_{21} & A_{22} \end{bmatrix}, \quad (14)$$

$$\left\{ \begin{array}{l} A_{11} = \frac{\dot{\tilde{S}}_u}{\tilde{S}_u} - \frac{\dot{\tilde{S}}_i}{\tilde{S}_i} - \frac{\tilde{I}r_1}{\tilde{E}_p} - (\omega_1^* + \rho_1) - \frac{\tilde{I}r_1}{\tilde{E}_p}(1 - \xi_1) - \omega_1^*, \quad A_{12} = \begin{bmatrix} 0 & 0 \end{bmatrix}, \\ A_{21} = \begin{bmatrix} (1 - \xi_1) \frac{\tilde{I}r_1}{\tilde{E}_p} \\ \frac{\tilde{I}r_1}{\tilde{E}_p} \end{bmatrix}, \quad A_{22} = \begin{bmatrix} x_{11} & x_{12} \\ x_{21} & x_{22} \end{bmatrix}, \quad x_{11} = \frac{\dot{\tilde{S}}_u}{\tilde{S}_u} - \frac{\dot{\tilde{S}}_i}{\tilde{S}_i} - 2\frac{\tilde{I}r_1}{\tilde{E}_p} - 2\omega_1^* - \rho_1 - \frac{\tilde{I}r_1}{\tilde{E}_p}\xi_1, \quad x_{12} = \rho_1, \\ x_{21} = \frac{\dot{\tilde{S}}_u}{\tilde{S}_u} - \frac{\dot{\tilde{S}}_i}{\tilde{S}_i} - \frac{\tilde{I}r_1}{\tilde{E}_p}(1 - \xi_1) - \omega_1^* - (\omega_1^* + \nu_1 + \eta_1), \quad x_{22} = \frac{\dot{\tilde{S}}_u}{\tilde{S}_u} - \frac{\dot{\tilde{S}}_i}{\tilde{S}_i} - \frac{\tilde{I}r_1}{\tilde{E}_p}(1 - \xi_1) - 2\omega_1^* - \nu_1 - \eta_1. \end{array} \right.$$

Let (b_1, b_2, b_3) be a vector in R^3 and $\|\cdot\|$ of (b_1, b_2, b_3) is specified by

$$\|b_1, b_2, b_3\| = \max \{\|b_1\| + \|b_2\| + \|b_3\|\}$$

Now we yield the Lozinski measure,

$$l(A) \leq \sup \{h_1, h_2\} = \sup \{l(A_{11}) + \|A_{12}\|, l(A_{22}) + \|A_{21}\|\}.$$

where $h_i = l(A_{ii}) + \|A_{ij}\|$, for $i = 1, 2$ and $i \neq j$, which implies that

$$h_1 = l(A_{11}) + \|A_{12}\|, \quad h_2 = l(A_{22}) + \|A_{21}\|. \quad (15)$$

where

$$l(A_{11}) = \frac{\dot{\tilde{S}}_u}{\tilde{S}_u} - \frac{\dot{\tilde{S}}_i}{\tilde{S}_i} - 2\frac{\tilde{I}r_1}{\tilde{E}_p} - 2\omega_1^* - \rho_1 - \frac{\tilde{I}r_1}{\tilde{E}_p}\xi_1$$

$$l(A_{22}) = \max \left\{ \frac{\dot{\tilde{S}}_u}{\tilde{S}_u} - \frac{\dot{\tilde{S}}_i}{\tilde{S}_i} - \frac{\tilde{I}r_1}{\tilde{E}_p}(1 - \xi_1) - \omega_1^* - (\omega_1^* + \nu_1 + \eta_1), \rho_1 \right\} = \left\{ \frac{\dot{\tilde{S}}_u}{\tilde{S}_u} - \frac{\dot{\tilde{S}}_i}{\tilde{S}_i} - \frac{\tilde{I}r_1}{\tilde{E}_p}(1 - \xi_1) - 2\omega_1^* - \nu_1 - \eta_1 \right\},$$

$$\|A_{12}\| = 0 \text{ and } \|A_{21}\| = \max \left\{ (1 - \xi_1) \frac{\tilde{I}r_1}{\tilde{E}_p}, \frac{\tilde{I}r_1}{\tilde{E}_p} \right\} = (1 - \xi_1) \frac{\tilde{I}r_1}{\tilde{E}_p}$$

Therefore, h_1 and h_2 becomes, such that

$$h_1 = \frac{\dot{\tilde{S}}_u}{\tilde{S}_u} - 2\omega_1^* - \nu_1 - \eta_1 \text{ and } h_2 = \frac{\dot{\tilde{S}}_u}{\tilde{S}_u} - (1 - \xi_1) - \min \{r - r\xi_1\}.$$

$$\text{This shows that } l(A) \leq \left\{ \frac{\dot{\tilde{S}}_u}{\tilde{S}_u} - (1 - \xi_1) - \min \{r - r\xi_1\} - 2\omega_1^* \right\}.$$

Hence, $l(A) \leq \frac{\dot{\tilde{S}}_u}{\tilde{S}_u} - (1 - \xi_1)$. Taking the integral of $l(A)$, one gets

$$\lim_{t \rightarrow \infty} \sup \sup \frac{1}{t} \int_0^t l(A) dt < -2\omega_1^*.$$

$$k = \lim_{t \rightarrow \infty} \sup \sup \frac{1}{t} \int_0^t l(A) dt < 0.$$

Hence, the model is globally asymptotically stable.

Theoretical exploration of the FO HIV dynamics

In this section, a fixed-point theorem is applied to determine the existence and uniqueness of the devised fractional-order model (5). This approach provides insights into the likelihood of a solution's existence. The relevant equation is derived by applying the generalized integral to one of the nodes in the model (5).

$$\tilde{S}_u(\hat{p}) - \tilde{S}_u(0) = I_{0+}^{\delta, \sigma} \left\{ X - \frac{\tilde{S}_u \tilde{I} \gamma_1}{\tilde{E}_p} - \tilde{S}_u(\omega_{(1)}^* + \rho_1) \right\},$$

$$\tilde{S}_i(\hat{p}) - \tilde{S}_i(0) = I_{0+}^{\delta, \sigma} \left\{ \tilde{S}_u \rho_1 - \frac{\tilde{S}_i \tilde{I} \gamma_1}{\tilde{E}_p} (1 - \xi_1) - \tilde{S}_i \omega_{(1)}^* \right\},$$

$$\tilde{I}(\hat{p}) - \tilde{I}(0) = I_{0+}^{\delta, \sigma} \left\{ (\tilde{S}_i(1 - \xi_1) + \tilde{S}_u) \frac{\tilde{I} \gamma_1}{\tilde{E}_p} + \tilde{C} \phi_{(1)} + \tilde{A} \theta_1 - \tilde{I}(\omega_{(1)}^* + \nu_1 + \eta_{(1)}) \right\}, \quad (16)$$

$$\tilde{A}(\hat{p}) - \tilde{A}(0) = I_{0+}^{\delta, \sigma} \left\{ \tilde{I} \eta_{(1)} - \tilde{A}(\varphi_1 + \omega_{(1)}^* + \theta_1) \right\}$$

,

$$\tilde{C}(\hat{p}) - \tilde{C}(0) = I_{0+}^{\delta, \sigma} \left\{ \tilde{I} \nu_1 - \tilde{C}(\omega_{(1)}^* + \phi_{(1)}) \right\}$$

,

$$\tilde{R}(\hat{p}) - \tilde{R}(0) = I_{0+}^{\delta, \sigma} \left\{ \tilde{I} \sigma_1 + \tilde{C} \sigma_2 + \tilde{A} \sigma_3 - \tilde{R} \omega_{(1)}^* \right\}$$

For clarity, the kernel is assumed as follows:

$$F_1(\hat{p}, \tilde{S}_u) = X - \frac{\tilde{S}_u \tilde{I} \gamma_1}{\tilde{E}_p} - \tilde{S}_u(\omega_{(1)}^* + \rho_1),$$

$$F_2(\hat{p}, \tilde{S}_i) = \tilde{S}_u \rho_1 - \frac{\tilde{S}_i \tilde{I} \gamma_1}{\tilde{E}_p} (1 - \xi_1) - \tilde{S}_i \omega_{(1)}^*,$$

$$F_3(\hat{p}, \tilde{I}) = (\tilde{S}_i(1 - \xi_1) + \tilde{S}_u) \frac{\tilde{I} \gamma_1}{\tilde{E}_p} + \tilde{C} \phi_{(1)} + \tilde{A} \theta_1 - \tilde{I}(\omega_{(1)}^* + \nu_1 + \eta_{(1)}), \quad (17)$$

$$F_4(\hat{p}, \tilde{A}) = \tilde{I} \eta_{(1)} - \tilde{A}(\varphi_1 + \omega_{(1)}^* + \theta_1),$$

$$F_5(\hat{p}, \tilde{C}) = \tilde{I} \nu_1 - \tilde{C}(\omega_{(1)}^* + \phi_{(1)}),$$

$$F_6(\hat{p}, \tilde{R}) = \tilde{I} \sigma_1 + \tilde{C} \sigma_2 + \tilde{A} \sigma_3 - \tilde{R} \omega_{(1)}^*.$$

Thus,

$$\begin{aligned} \tilde{S}_u(\hat{p}) - \tilde{S}_u(0) &= \frac{\sigma^{(1-\delta)}}{\Gamma(\delta)} \int_0^{\hat{p}} \xi^{(\delta-1)} (\hat{p}^\sigma - \xi^\sigma)^{\delta-1} F_1(\xi, \tilde{S}_u) d\xi, \\ \tilde{S}_i(\hat{p}) - \tilde{S}_i(0) &= \frac{\sigma^{(1-\delta)}}{\Gamma(\delta)} \int_0^{\hat{p}} \xi^{(\delta-1)} (\hat{p}^\sigma - \xi^\sigma)^{\delta-1} F_2(\xi, \tilde{S}_i) d\xi, \\ \tilde{I}(\hat{p}) - \tilde{I}(0) &= \frac{\sigma^{(1-\delta)}}{\Gamma(\delta)} \int_0^{\hat{p}} \xi^{(\delta-1)} (\hat{p}^\sigma - \xi^\sigma)^{\delta-1} F_3(\xi, \tilde{I}) d\xi, \\ \tilde{A}(\hat{p}) - \tilde{A}(0) &= \frac{\sigma^{(1-\delta)}}{\Gamma(\delta)} \int_0^{\hat{p}} \xi^{(\delta-1)} (\hat{p}^\sigma - \xi^\sigma)^{\delta-1} F_4(\xi, \tilde{A}) d\xi, \\ \tilde{C}(\hat{p}) - \tilde{C}(0) &= \frac{\sigma^{(1-\delta)}}{\Gamma(\delta)} \int_0^{\hat{p}} \xi^{(\delta-1)} (\hat{p}^\sigma - \xi^\sigma)^{\delta-1} F_5(\xi, \tilde{C}) d\xi, \\ \tilde{R}(\hat{p}) - \tilde{R}(0) &= \frac{\sigma^{(1-\delta)}}{\Gamma(\delta)} \int_0^{\hat{p}} \xi^{(\delta-1)} (\hat{p}^\sigma - \xi^\sigma)^{\delta-1} F_6(\xi, \tilde{R}) d\xi. \end{aligned} \quad (18)$$

Theorem 5.1 The kernel's F_1, F_2, F_3, F_4, F_5 and F_6 fulfil the subsequent inequality exists if the contraction and Lipschitz condition accomplished as

$$0 \leq \Delta_1, \Delta_2, \Delta_3, \Delta_4, \Delta_5, \Delta_6 < 1.$$

Proof Since \tilde{S}_u and \tilde{S}_u^* for kernel F_1 , yields

$$\|F_1(\hat{p}, \tilde{S}_u) - F_1(\hat{p}, \tilde{S}_u^*)\| = \left\| -\left(\frac{\tilde{I}\gamma_1}{\tilde{E}_p} + (\omega_{(1)}^* + \rho_1)\right)(\tilde{S}_u - \tilde{S}_u^*) \right\|, \quad (19)$$

$$\begin{aligned} \|F_1(\hat{p}, \tilde{S}_u) - F_1(\hat{p}, \tilde{S}_u^*)\| &\leq \left(\frac{\|\tilde{I}\| \gamma_1}{\tilde{E}_p} + \omega_{(1)}^* + \rho_1\right) \|\tilde{S}_u - \tilde{S}_u^*\|, \\ &\leq \left(\frac{m_3 \gamma_1}{\tilde{E}_p} + \omega_{(1)}^* + \rho_1\right) \|\tilde{S}_u - \tilde{S}_u^*\|, \\ &\leq \Delta_1 \|\tilde{S}_u - \tilde{S}_u^*\|. \end{aligned} \quad (20)$$

Here, it is supposed $\Delta_1 = \frac{k_3 \gamma_1}{\tilde{E}_p} + \omega_{(1)}^* + \rho_1 < 1$ and $\|\tilde{I}\| \leq k_3$ be the bounded function. Therefore, one obtains

$$\|F_1(\hat{p}, \tilde{S}_u) - F_1(\hat{p}, \tilde{S}_u^*)\| \leq \Delta_1 \|\tilde{S}_u - \tilde{S}_u^*\|. \quad (21)$$

The kernel F_1 fulfills the Lipschitz conditions (LC) then $0 < \Delta_1 < 1$, so the criterion for contraction F_1 is also valid. Additionally, inequality for subsequent kernels is obtained as:

$$\begin{aligned} \|F_2(\hat{p}, \tilde{S}_i) - F_2(\hat{p}, \tilde{S}_i^*)\| &\leq \Delta_2 \|\tilde{S}_i - \tilde{S}_i^*\|. \\ \|F_3(\hat{p}, \tilde{I}) - F_3(\hat{p}, \tilde{I}^*)\| &\leq \Delta_3 \|\tilde{I} - \tilde{I}^*\|. \\ \|F_4(\hat{p}, \tilde{A}) - F_4(\hat{p}, \tilde{A}^*)\| &\leq \Delta_4 \|\tilde{A} - \tilde{A}^*\|, \\ \|F_5(\hat{p}, \tilde{C}) - F_5(\hat{p}, \tilde{C}^*)\| &\leq \Delta_5 \|\tilde{C} - \tilde{C}^*\|. \\ \|F_6(\hat{p}, \tilde{R}) - F_6(\hat{p}, \tilde{R}^*)\| &\leq \Delta_6 \|\tilde{R} - \tilde{R}^*\|. \end{aligned} \quad (22)$$

Now implement the recursive formula on Eq. (8), one gets.

$$\begin{aligned} \tilde{S}_{u_l}(\hat{p}) &= \tilde{S}_u(0) + \frac{\sigma^{(1-\delta)}}{\Gamma(\delta)} \int_0^{\hat{p}} \xi^{(\delta-1)} (\hat{p}^\sigma - \xi^\sigma)^{\delta-1} F_1(\xi, \tilde{S}_{u_{(l-1)}}) d\xi, \\ \tilde{S}_{i_l}(\hat{p}) &= \tilde{S}_i(0) + \frac{\sigma^{(1-\delta)}}{\Gamma(\delta)} \int_0^{\hat{p}} \xi^{(\delta-1)} (\hat{p}^\sigma - \xi^\sigma)^{\delta-1} F_2(\xi, \tilde{S}_{i_{(l-1)}}) d\xi, \\ \tilde{I}_l(\hat{p}) &= \tilde{I}(0) + \frac{\sigma^{(1-\delta)}}{\Gamma(\delta)} \int_0^{\hat{p}} \xi^{(\delta-1)} (\hat{p}^\sigma - \xi^\sigma)^{\delta-1} F_3(\xi, \tilde{I}_{(l-1)}) d\xi, \\ \tilde{C}_l(\hat{p}) &= \tilde{C}(0) + \frac{\sigma^{(1-\delta)}}{\Gamma(\delta)} \int_0^{\hat{p}} \xi^{(\delta-1)} (\hat{p}^\sigma - \xi^\sigma)^{\delta-1} F_4(\xi, \tilde{C}_{(l-1)}) d\xi, \\ \tilde{A}_l(\hat{p}) &= \tilde{A}(0) + \frac{\sigma^{(1-\delta)}}{\Gamma(\delta)} \int_0^{\hat{p}} \xi^{(\delta-1)} (\hat{p}^\sigma - \xi^\sigma)^{\delta-1} F_5(\xi, \tilde{A}_{(l-1)}) d\xi, \\ \tilde{R}_l(\hat{p}) &= \tilde{R}(0) + \frac{\sigma^{(1-\delta)}}{\Gamma(\delta)} \int_0^{\hat{p}} \xi^{(\delta-1)} (\hat{p}^\sigma - \xi^\sigma)^{\delta-1} F_6(\xi, \tilde{R}_{(l-1)}) d\xi, \end{aligned} \quad (23)$$

So, the initial conditions are given as per:

$$\tilde{S}_u(\hat{p}_0) = \tilde{S}_u(0), \tilde{S}_i(\hat{p}_0) = \tilde{S}_i(0), \tilde{I}(\hat{p}_0) = \tilde{I}(0), \tilde{C}(\hat{p}_0) = \tilde{C}(0), \tilde{A}(\hat{p}_0) = \tilde{A}(0), \tilde{R}(\hat{p}_0) = \tilde{R}(0).$$

Furthermore, by computing the difference between successive terms, the following lexis are obtained:

$$\begin{aligned}
\psi_l(\hat{p}) &= \tilde{S}_{u_l}(\hat{p}) - \tilde{S}_{u_{(l-1)}}(\hat{p}) = \frac{\sigma^{(1-\delta)}}{\Gamma(\delta)} \int_0^{\hat{p}} \xi^{(\delta-1)} (\hat{p}^\sigma - \xi^\sigma)^{\delta-1} (F_1(\xi, \tilde{S}_{u_{(l-1)}}) - F_1(\xi, \tilde{S}_{u_{(l-2)}})) d\xi, \\
\xi_l(\hat{p}) &= \tilde{S}_{i_l}(\hat{p}) - \tilde{S}_{i_{(l-1)}}(\hat{p}) = \frac{\sigma^{(1-\delta)}}{\Gamma(\delta)} \int_0^{\hat{p}} \xi^{(\delta-1)} (\hat{p}^\sigma - \xi^\sigma)^{\delta-1} (F_2(\xi, \tilde{S}_{i_{(l-1)}}) - F_2(\xi, \tilde{S}_{i_{(l-2)}})) d\xi, \\
\phi_l(\hat{p}) &= \tilde{I}_l(\hat{p}) - \tilde{I}_{(l-1)}(\hat{p}) = \frac{\sigma^{(1-\delta)}}{\Gamma(\delta)} \int_0^{\hat{p}} \xi^{(\delta-1)} (\hat{p}^\sigma - \xi^\sigma)^{\delta-1} (F_3(\xi, \tilde{I}_{(l-1)}) - (F_3(\xi, \tilde{I}_{(l-2)}))) d\xi, \quad (24) \\
\chi_l(\hat{p}) &= \tilde{A}_l(\hat{p}) - \tilde{A}_{(l-1)}(\hat{p}) = \frac{\sigma^{(1-\delta)}}{\Gamma(\delta)} \int_0^{\hat{p}} \xi^{(\delta-1)} (\hat{p}^\sigma - \xi^\sigma)^{\delta-1} (F_4(\xi, \tilde{A}_{(l-1)}) - F_4(\xi, \tilde{A}_{(l-2)})) d\xi, \\
\theta_l(\hat{p}) &= \tilde{C}_l(\hat{p}) - \tilde{C}_{(l-1)}(\hat{p}) = \frac{\sigma^{(1-\delta)}}{\Gamma(\delta)} \int_0^{\hat{p}} \xi^{(\delta-1)} (\hat{p}^\sigma - \xi^\sigma)^{\delta-1} (F_5(\xi, \tilde{C}_{(l-1)}) - F_5(\xi, \tilde{C}_{(l-2)})) d\xi, \\
\varphi_l(\hat{p}) &= \tilde{R}_l(\hat{p}) - \tilde{R}_{(l-1)}(\hat{p}) = \frac{\sigma^{(1-\delta)}}{\Gamma(\delta)} \int_0^{\hat{p}} \xi^{(\delta-1)} (\hat{p}^\sigma - \xi^\sigma)^{\delta-1} (F_6(\xi, \tilde{R}_{(l-1)}) - F_6(\xi, \tilde{R}_{(l-2)})) d\xi. \\
\tilde{S}_{u_l}(\hat{p}) &= \sum_{i=1}^l \psi_i(\hat{p}), \tilde{S}_{i_l}(\hat{p}) = \sum_{i=1}^l \xi_i(\hat{p}), \tilde{I}_l(\hat{p}) = \sum_{i=1}^l \phi_i(\hat{p}), \tilde{A}_l(\hat{p}) = \sum_{i=1}^l \chi_i(\hat{p}), \tilde{C}_l(\hat{p}) = \sum_{i=1}^l \theta_i(\hat{p}), \tilde{R}_l(\hat{p}) = \sum_{i=1}^l \varphi_i(\hat{p}).
\end{aligned}$$

Using the triangle inequality and Eq. (24) in norm form, after that, Eq. (24) is transformed into

$$\begin{aligned}
\| \psi_l(\hat{p}) \| &= \| \tilde{S}_{u_l}(\hat{p}) - \tilde{S}_{u_{(l-1)}}(\hat{p}) \| \\
&\leq \frac{\sigma^{(1-\delta)}}{\Gamma(\delta)} \left\| \int_0^{\hat{p}} \xi^{(\delta-1)} (\hat{p}^\sigma - \xi^\sigma)^{\delta-1} (F_1(\xi, \tilde{S}_{u_{(l-1)}}) - F_1(\xi, \tilde{S}_{u_{(l-2)}})) d\xi \right\|. \quad (25)
\end{aligned}$$

With the kernel LC, one attains;

$$\| \tilde{S}_{u_l}(\hat{p}) - \tilde{S}_{u_{(l-1)}}(\hat{p}) \| \leq \frac{\Delta_1 \sigma^{(1-\delta)}}{\Gamma(\delta)} \int_0^{\hat{p}} \xi^{(\delta-1)} (\hat{p}^\sigma - \xi^\sigma)^{\delta-1} \| \tilde{S}_{u_{(l-1)}}(\hat{p}) - \tilde{S}_{u_{(l-2)}}(\hat{p}) \| d\xi. \quad (26)$$

Therefore, the following result is obtained: $\| \psi_l(\hat{p}) \| \leq \frac{\Delta_1 \sigma^{(1-\delta)}}{\Gamma(\delta)} \int_0^{\hat{p}} \xi^{(\delta-1)} (\hat{p}^\sigma - \xi^\sigma)^{\delta-1} \| \psi_{(l-1)}(\xi) \| d\xi.$ (27)

In a similar manner, the subsequent expressions are obtained:

$$\| \xi_l(\hat{p}) \| \leq \frac{\Delta_2 \sigma^{(1-\delta)}}{\Gamma(\delta)} \int_0^{\hat{p}} \xi^{(\delta-1)} (\hat{p}^\sigma - \xi^\sigma)^{\delta-1} \| \xi_{(l-1)}(\xi) \| d\xi.$$

$$\| \phi_l(\hat{p}) \| \leq \frac{\Delta_3 \sigma^{(1-\delta)}}{\Gamma(\delta)} \int_0^{\hat{p}} \xi^{(\delta-1)} (\hat{p}^\sigma - \xi^\sigma)^{\delta-1} \| \phi_{(l-1)}(\xi) \| d\xi. \quad (27)$$

$$\| \chi_l(\hat{p}) \| \leq \frac{\Delta_4 \sigma^{(1-\delta)}}{\Gamma(\delta)} \int_0^{\hat{p}} \xi^{(\delta-1)} (\hat{p}^\sigma - \xi^\sigma)^{\delta-1} \| \chi_{(l-1)}(\xi) \| d\xi.$$

$$\| \theta_l(\hat{p}) \| \leq \frac{\Delta_5 \sigma^{(1-\delta)}}{\Gamma(\delta)} \int_0^{\hat{p}} \xi^{(\delta-1)} (\hat{p}^\sigma - \xi^\sigma)^{\delta-1} \| \theta_{(l-1)}(\eta) \| d\eta.$$

$$\| \varphi_l(\hat{p}) \| \leq \frac{\Delta_6 \sigma^{(1-\delta)}}{\Gamma(\delta)} \int_0^{\hat{p}} \xi^{(\delta-1)} (\hat{p}^\sigma - \xi^\sigma)^{\delta-1} \| \varphi_{(l-1)}(\xi) \| d\xi.$$

Theorem 5.2 The considered system (5) has a solution if there exists a value t_{\max}^σ such that

$$\frac{\Delta_1}{\Gamma(\delta+1)} \left(\frac{t_{\max}^\sigma}{\sigma} \right)^\delta < 1.$$

Proof It is acknowledged that the functions $\tilde{S}_u(\hat{t})$, $\tilde{S}_i(\hat{t})$, $\tilde{I}(\hat{t})$, $\tilde{C}(\hat{t})$, $\tilde{A}(\hat{t})$ and $\tilde{R}(\hat{t})$ are bounded then kernels fulfill the LC as well. Therefore, the following relations may be found by using provided Eq. (5.12) and (5.13)

$$\begin{aligned} \| \psi_l(\hat{p}) \| &\leq \| \tilde{S}_u(0) \| \left[\frac{\Delta_1}{\Gamma(\delta+1)} \left(\frac{\hat{p}_{\max}^\sigma}{\sigma} \right)^\delta \right]^l, \\ \| \xi_l(\hat{p}) \| &\leq \| S_i(0) \| \left[\frac{\Delta_2}{\Gamma(\delta+1)} \left(\frac{\hat{p}_{\max}^\sigma}{\sigma} \right)^\delta \right]^l, \\ \| \phi_l(\hat{p}) \| &\leq \| \tilde{I}(0) \| \left[\frac{\Delta_3}{\Gamma(\delta+1)} \left(\frac{\hat{p}_{\max}^\sigma}{\sigma} \right)^\delta \right]^l, \\ \| \chi_n(\hat{p}) \| &\leq \| \tilde{A}(0) \| \left[\frac{\Delta_4}{\Gamma(\delta+1)} \left(\frac{\hat{p}_{\max}^\sigma}{\sigma} \right)^\delta \right]^l, \\ \| \theta_l(\hat{p}) \| &\leq \| \tilde{C}(0) \| \left[\frac{\Delta_5}{\Gamma(\delta+1)} \left(\frac{\hat{p}_{\max}^\sigma}{\sigma} \right)^\delta \right]^l, \\ \| \varphi_l(\hat{p}) \| &\leq \| \tilde{R}(0) \| \left[\frac{\Delta_6}{\Gamma(\delta+1)} \left(\frac{\hat{p}_{\max}^\sigma}{\sigma} \right)^\delta \right]^l. \end{aligned} \quad (28)$$

Consequently, the model's solution is real and continuous. To demonstrate that the function represents the system's solutions, the assumption is made.

$$\begin{aligned} \tilde{S}_u(\hat{p}) - \tilde{S}_u(0) &= \tilde{S}_{u_n}(\hat{p}) - H_l^1(\hat{p}), \\ \tilde{S}_i(\hat{p}) - \tilde{S}_i(0) &= \tilde{S}_{i_l}(\hat{p}) - H_l^2(\hat{p}), \\ \tilde{I}(\hat{p}) - \tilde{I}(0) &= \tilde{I}_l(\hat{p}) - H_l^3(\hat{p}), \\ \tilde{A}(\hat{p}) - \tilde{A}(0) &= \tilde{A}_l(\hat{p}) - H_l^4(\hat{p}), \\ \tilde{C}(\hat{p}) - \tilde{C}(0) &= \tilde{C}_l(\hat{p}) - H_l^5(\hat{p}), \\ \tilde{R}(\hat{p}) - \tilde{R}(0) &= \tilde{R}_l(\hat{p}) - H_l^6(\hat{p}). \end{aligned} \quad (29)$$

Since our purpose is to demonstrate that while $l \rightarrow \infty$ the factor $\| H_l^1(t) \|$ turns to zero. Taking the standard LC for the kernel F_1 , provides,

$$\begin{aligned} \| H_l^1(\hat{p}) \| &\leq \frac{\sigma^{(1-\delta)}}{\Gamma(\delta)} \int_0^{\hat{p}} \xi^{(\delta-1)} (\hat{p}^\sigma - \xi^\sigma)^{\delta-1} (F_1(\xi, \tilde{S}_u) - F_1(\xi, \tilde{S}_{u_{(l-1)}})) d\xi, \\ &\leq \frac{\sigma^{(1-\delta)}}{\Gamma(\delta)} \int_0^{\hat{p}} \xi^{(\delta-1)} (\hat{p}^\sigma - \xi^\sigma)^{\delta-1} \| (F_1(\xi, \tilde{S}_u) - F_1(\xi, \tilde{S}_{u_{(l-1)}})) \| d\xi, \\ &\leq \frac{\Delta_1}{\Gamma(\delta+1)} \left(\frac{\hat{p}^\sigma}{\sigma} \right)^\delta \| \tilde{S}_u - \tilde{S}_{u_{(l-1)}} \|. \end{aligned} \quad (30)$$

Then, by repeating the same steps once more, the following result is obtained:

$$\| H_l^1(\hat{p}) \| \leq \| \tilde{S}_u(0) \| \left[\frac{1}{\Gamma(\delta+1)} \left(\frac{\hat{p}^\sigma}{\sigma} \right)^\delta \right]^{(l+1)} \Delta_1^l E, \quad (31)$$

at \hat{p}_{\max} , yields

$$\| H_l^1(\hat{p}) \| \leq \| \tilde{S}_l(0) \| \left[\frac{1}{\Gamma(\delta+1)} \left(\frac{\hat{p}_{\max}^\sigma}{\sigma} \right)^\delta \right]^{(l+1)} \Delta_1^l E. \quad (32)$$

Taking the limit $l \rightarrow \infty$, on Eq. (33), yields $\|H_l^1(\hat{p})\| \rightarrow 0$. Correspondingly, the following result can be attained: $\|H_l^2(\hat{p})\|$, $\|H_l^3(\hat{p})\|$, $\|H_l^4(\hat{p})\|$, $\|H_l^5(\hat{p})\|$, and $\|H_l^6(\hat{p})\|$ tend to 0.

Another crucial component is proving that model solutions are unique. Because of this, it is inferred from the contradiction that alternative forms exist, $\tilde{S}_u^*(\hat{t})$, $\tilde{I}^*(\hat{t})$, $\tilde{C}^*(\hat{t})$, $\tilde{S}_a^*(\hat{t})$, $\tilde{A}^*(\hat{t})$ and $\tilde{R}^*(\hat{t})$ then

$$\tilde{S}_u(\hat{p}) - \tilde{S}_u^*(\hat{p}) \leq \frac{\sigma^{(1-\delta)}}{\Gamma(\delta)} \int_0^{\hat{p}} \xi^{(\sigma-1)} (\hat{p}^\sigma - \xi^\sigma)^{\delta-1} (F_1(\xi, \tilde{S}_u) - F_1(\xi, \tilde{S}_u^*)) d\xi. \quad (33)$$

By applying the norm to Eq. (34), the following result is gained:

$$\|\tilde{S}_u(\hat{p}) - \tilde{S}_u^*(\hat{p})\| \leq \frac{\sigma^{(1-\delta)}}{\Gamma(\delta)} \int_0^{\hat{p}} \xi^{(\sigma-1)} (\hat{p}^\sigma - \xi^\sigma)^{\delta-1} \|F_1(\xi, \tilde{S}_u) - F_1(\xi, \tilde{S}_u^*)\| d\xi, \quad (34)$$

By extending LC to kernels, the following result is attained:

$$\|\tilde{S}_u(\hat{p}) - \tilde{S}_u^*(\hat{p})\| \leq \frac{\Delta_1}{\Gamma(\delta+1)} \left(\frac{\hat{p}^\sigma}{\sigma}\right)^\delta \|\tilde{S}_u(\hat{p}) - \tilde{S}_u^*(\hat{p})\|, \quad (35)$$

$$\|\tilde{S}_u(\hat{p}) - \tilde{S}_u^*(\hat{p})\| \left[1 - \frac{\Delta_1}{\Gamma(\delta+1)} \left(\frac{\hat{p}^\sigma}{\sigma}\right)^\delta\right] \leq 0, \quad (36)$$

$$\|\tilde{S}_u(\hat{p}) - \tilde{S}_u^*(\hat{p})\| = 0, \rightarrow \tilde{S}_u(\hat{p}) = \tilde{S}_u^*(\hat{p}). \quad (37)$$

Thus, the uniqueness of the devised system's solution is established. Consequently, it is shown that

$$\begin{aligned} \tilde{S}_u(\hat{p}) &= \tilde{S}_u^*(\hat{p}), \tilde{S}_i(\hat{p}) = \tilde{S}_i^*(\hat{p}), \tilde{I}(\hat{p}) = \tilde{I}^*(\hat{p}), \tilde{A}(\hat{p}) = \tilde{A}^*(\hat{p}), \tilde{C}(\hat{p}) = \tilde{C}^*(\hat{p}), \\ \tilde{R}(\hat{p}) &= \tilde{R}^*(\hat{p}). \end{aligned} \quad (38)$$

Numerical techniques for the devised model

When all other existing analytical methods fail, numerical techniques are employed to find a solution. Numerical approaches are considered the most suitable method for representing solutions to models using fractional-order calculus. In this section, the newly adaptive Predictor–Corrector (P–C) approach is presented, anticipated by⁴ beneath the Generalized Caputo Operator (GCO), which extends the P–C method outlined in⁵. Consider the initial value problem (IVP) stated as:

$$\begin{aligned} {}^C D_{a+}^{\delta, \sigma} z(\hat{p}) &= f(t, Z(\hat{p})), \quad \hat{p} \in [0, T], \\ Z^l(a) &= Z_0^l, \quad l = 0, 1, \dots, [\delta]. \end{aligned} \quad (39)$$

where $\delta \in ((k-1), k]$, $a \geq 0$, and $\sigma > 0$. Through applying the generalized integral, Eq. (40) can be stated as a Volterra integral equation:

$$Z(\hat{p}) = q(\hat{p}) + \frac{\sigma^{(1-\delta)}}{\Gamma(\delta)} \int_a^{\hat{p}} \xi^{(\sigma-1)} (\hat{p}^\sigma - \xi^\sigma)^{\delta-1} f(\xi, Z(\xi)) d\xi. \quad (40)$$

$$\text{where, } q(\hat{p}) = \sum_{r=0}^{(k-1)} \frac{1}{\sigma^r r!} (\hat{p}^\sigma - a^\sigma)^r [(x^{1-\sigma} \frac{d}{dx})^r Z(x)]|_{x=a}.$$

Based on the theory, the first stage in our method is where the function Z such that there is a unique solution on a certain interval $[a, \hat{P}]$, comprises of splitting the interval $[a, \hat{P}]$ into N subintervals $\{\hat{p}_l, \hat{p}_{l+1}\}$, $l = 0, 1, \dots, N-1$ integrating the mesh points:

$$\begin{aligned} \hat{p}_0 &= a, \\ \hat{p}_{l+1} &= (\hat{p}_l^\sigma + h)^\frac{1}{\sigma}, \quad l = 0, 1, \dots, (N-1), \end{aligned} \quad (41)$$

where $h = \frac{(\hat{P}^\sigma - a^\sigma)}{N}$ and natural number is N . To solve our devised initial value problem numerically, Now, the approximation will be extended Z_l , $l = 0, 1, \dots, N$. The fundamental behavior, assuming that the previous investigation of the estimation has been conducted $Z_w \approx Z(\hat{p}_w)$, $w = 1, 2, \dots, n$, is that an estimate solution needs to be obtained $Z_{(l+1)} \approx Z(\hat{p}_{(l+1)})$ with an integral equation

$$Z(\hat{p}_{(l+1)}) = q(\hat{p}_{(l+1)}) + \frac{\sigma^{(1-\delta)}}{\Gamma(\delta)} \int_a^{\hat{p}_{(l+1)}} \xi^{(\sigma-1)} (\hat{p}_{l+1}^\sigma - \xi^\sigma)^{\delta-1} f(\xi, Z(\xi)) d\xi, \quad (42)$$

By substitution $\eta^\sigma = \lambda$, one get

$$Z(\hat{p}_{(l+1)}) = q(\hat{p}_{(l+1)}) + \frac{\sigma^{(-\delta)}}{\Gamma(\delta)} \int_{a^\sigma}^{\hat{p}_{(l+1)}^\sigma} (\hat{p}_{l+1}^\sigma - \lambda)^{\delta-1} f(\lambda^{\frac{1}{\sigma}}, Z(\lambda^{\frac{1}{\sigma}})) d\lambda, \quad (43)$$

$$Z(\hat{p}_{(l+1)}) = q(\hat{p}_{(l+1)}) + \frac{\sigma^{(-\delta)}}{\Gamma(\delta)} \sum_{j=0}^l \int_{t_j^\sigma}^{\hat{p}_{(j+1)}^\sigma} (\hat{p}_{l+1}^\sigma - \lambda)^{\delta-1} f(\lambda^{\frac{1}{\sigma}}, Z(\lambda^{\frac{1}{\sigma}})) d\lambda. \quad (44)$$

Then, if the weight function-related trapezoidal quadrature rule is utilized $(\hat{p}_{(l+1)}^\sigma - \lambda)^{\delta-1}$ to replace the function with an approximation integral on the right-hand sides of (6.6) $f(\lambda^{\frac{1}{\sigma}}, Z(\lambda^{\frac{1}{\sigma}}))$ using its piecewise linear interpolator and suitable nodes at the \hat{p}_w^σ ($w = 0, 1, \dots, (l+1)$), then one obtain,

$$\begin{aligned} \int_{t_w^\sigma}^{\hat{p}_{(w+1)}^\sigma} (\hat{p}_{(l+1)}^\sigma - \lambda)^{(\delta-1)} f(\lambda^{\frac{1}{\sigma}}, Z(\lambda^{\frac{1}{\sigma}})) d\lambda &\approx \frac{h^{(\delta)}}{\delta(\delta+1)} \{((l-w)^{(\delta+1)} - (l-w-\delta) \\ &((l-(w+1))^\delta) f(\hat{p}_{(w)}, Z(\hat{p}_{(w)})) + ((l-w+1)^{\delta+1} \\ &-(l-(w)+\delta+1)(l-(w))^\delta f(\hat{p}_{(w+1)}, Z(\hat{p}_{(w+1)}))\}. \end{aligned} \quad (45)$$

The corrector formulae for the function $Z(\hat{p}_{(l+1)})$, $l = 0, 1, \dots, N-1$, are attained from (46) and (47) and are documented as follows:

$$Z(\hat{p}_{(l+1)}) \approx q(\hat{p}_{(l+1)}) + \frac{\sigma^{(-\delta)} h^{(\delta)}}{\Gamma(\delta+2)} \sum_{j=0}^{(l)} \nabla_{j, (l+1)} f(\hat{p}_w, Z(\hat{p}_w)) + \frac{\sigma^{(-\delta)} h^{(\delta)}}{\Gamma(\delta+2)} f(\hat{p}_{(l+1)}, Z(\hat{p}_{(l+1)})). \quad (46)$$

When the weight function appears $\nabla_{w, (l+1)}$ is described as:

$$\nabla_{w, (l+1)} = \frac{l^{(\delta+1)} - (l-\delta)(l+1)^\delta}{(l-w+2)^{(\delta+1)} + (l-w)^{(\delta+1)} - 2(l-w+1)^{(\delta+1)}}, \quad \text{if } \begin{matrix} w=0 \\ 1 \leq (w) \leq l. \end{matrix} \quad (47)$$

Now, utilizing our approach on the quantity $Z(\hat{p}_{(l+1)})$ provides the quantity $Z^P(\hat{p}_{(l+1)})$ in (47) which is known as predictor value. It is also attainable from (44) using the Adams-Bashforth approach. In this regard, $f(\lambda^{\frac{1}{\sigma}}, Z(\lambda^{\frac{1}{\sigma}}))$ substituted by $f(\hat{p}_{(w)}, Z(\hat{p}_{(w)}))$ in (45) on every integral, then the predictor value $Z^P(\hat{p}_{(l+1)}) \approx Z^P(\hat{p}_{(l+1)})$ is obtained as per:

$$\begin{aligned} Z_{(l+1)}^P &\approx q(\hat{p}_{(l+1)}) + \frac{\sigma^{-\delta}}{\Gamma(\delta)} \sum_{w=0}^l \int_{t_{(w)}^\sigma}^{\hat{p}_{(w+1)}^\sigma} (\hat{p}_{l+1}^\sigma - \lambda)^{(\delta-1)} f(\hat{p}_{(w)}, Z(\hat{p}_{(w)})) d\lambda, \\ &= q(\hat{p}_{(l+1)}) + \frac{\sigma^{(-\delta)} h^{(\delta)}}{\Gamma(\delta+1)} \sum_{w=0}^{(l)} \Pi_{w, (l+1)} f(\hat{p}_{(w)}, Z(\hat{p}_{(w)})). \end{aligned} \quad (48)$$

where,

$$\Pi_{w, (l+1)} = [(l+1-(w))^\delta - (l-w)^\delta] 0 \leq w \leq l.$$

Consequently, the Adaptive-P-C method for assessing estimation $Z_{(l+1)} \approx Z(\hat{p}_{(l+1)})$ is completely indicated by the formula

$$Z_{(l+1)} \approx q(\hat{p}_{(l+1)}) + \frac{\sigma^{(-\alpha)} h^{(\alpha)}}{\Gamma(\alpha+2)} \sum_{w=0}^{(l)} \nabla_{w, l+1} f(\hat{p}_{(w)}, Z(\hat{p}_{(w)})) + \frac{\sigma^{(-\alpha)} h^{(\alpha)}}{\Gamma(\alpha+2)} f(\hat{p}_{(l+1)}, Z_{(l+1)}^P). \quad (49)$$

Diethelm et al.²⁵ offered where $\sigma = 1$, the A-P-C technique is dropped to decrease to P-C approach.

Adaptive P–C approach for modeling HIV/AIDS propagation within a fractional-order framework

The estimation of the corrected values is now implemented $\tilde{S}_{u(l+1)}, \tilde{S}_{i(l+1)}, \tilde{I}_{(l+1)}, \tilde{A}_{(l+1)}, \tilde{C}_{(l+1)}$ in the implied model (4) to perform the Adaptive-P-C approach:

$$\begin{aligned}
 \tilde{S}_{u(l+1)} &\approx E_1 + \frac{\sigma^{(-\delta)} h^{(\delta)}}{\Gamma(\delta+2)} \sum_{w=0}^{(l)} \nabla_{w,(l+1)} B_1(\hat{p}_{(w)}, \tilde{S}_{u(w)}, \tilde{S}_{i(w)}, \tilde{I}_{(w)}, \tilde{A}_{(w)}, \tilde{C}_{(w)}, \tilde{R}_{(w)}) \\
 &+ \frac{\sigma^{(-\delta)} h^{(\delta)}}{\Gamma(\delta+2)} B_1(\hat{p}_{(l+1)}, \tilde{S}_{u(l+1)}^P, \tilde{S}_{i(l+1)}^P, \tilde{I}_{(l+1)}^P, \tilde{A}_{(l+1)}^P, \tilde{C}_{(l+1)}^P, \tilde{R}_{(l+1)}^P), \\
 \tilde{S}_{i(l+1)} &\approx E_2 + \frac{\sigma^{(-\delta)} h^{(\delta)}}{\Gamma(\delta+1)} \sum_{w=0}^{(l)} \nabla_{w,(l+1)} B_2(\hat{p}_{(w)}, \tilde{S}_{u(w)}, \tilde{S}_{i(w)}, \tilde{I}_{(w)}, \tilde{A}_{(w)}, \tilde{C}_{(w)}, \tilde{R}_{(w)}) \\
 &+ \frac{\sigma^{(-\delta)} h^{(\delta)}}{\Gamma(\delta+1)} B_2(\hat{p}_{(l+1)}, \tilde{S}_{u(l+1)}^P, \tilde{S}_{i(l+1)}^P, \tilde{I}_{(l+1)}^P, \tilde{A}_{(l+1)}^P, \tilde{C}_{(l+1)}^P, \tilde{R}_{(l+1)}^P), \\
 \tilde{I}_{(l+1)} &\approx E_3 + \frac{\sigma^{(-\delta)} h^{(\delta)}}{\Gamma(\delta+1)} \sum_{w=0}^{(l)} \nabla_{w,(l+1)} B_3(\hat{p}_{(w)}, \tilde{S}_{u(w)}, \tilde{S}_{i(w)}, \tilde{I}_{(w)}, \tilde{A}_{(w)}, \tilde{C}_{(w)}, \tilde{R}_{(w)}) \\
 &+ \frac{\sigma^{(-\delta)} h^{(\delta)}}{\Gamma(\delta+1)} B_3(\hat{p}_{(l+1)}, \tilde{S}_{u(l+1)}^P, \tilde{S}_{i(l+1)}^P, \tilde{I}_{(l+1)}^P, \tilde{A}_{(l+1)}^P, \tilde{C}_{(l+1)}^P, \tilde{R}_{(l+1)}^P), \\
 \tilde{A}_{(l+1)} &\approx E_4 + \frac{\sigma^{(-\delta)} h^{(\delta)}}{\Gamma(\delta+2)} \sum_{w=0}^{(l)} \nabla_{w,l+1} B_4(\hat{p}_{(w)}, \tilde{S}_{u(w)}, \tilde{S}_{i(w)}, \tilde{I}_{(w)}, \tilde{A}_{(w)}, \tilde{C}_{(w)}, \tilde{R}_{(w)}) \\
 &+ \frac{\sigma^{(-\delta)} h^{(\delta)}}{\Gamma(\delta+2)} B_4(\hat{p}_{(l+1)}, \tilde{S}_{u(l+1)}^P, \tilde{S}_{i(l+1)}^P, \tilde{I}_{(l+1)}^P, \tilde{A}_{(l+1)}^P, \tilde{C}_{(l+1)}^P, \tilde{R}_{(l+1)}^P), \\
 \tilde{C}_{(l+1)} &\approx E_5 + \frac{\sigma^{(-\delta)} h^{(\delta)}}{\Gamma(\delta+2)} \sum_{w=0}^{(l)} \nabla_{w,(l+1)} B_5(\hat{p}_{(w)}, \tilde{S}_{u(w)}, \tilde{S}_{i(w)}, \tilde{I}_{(w)}, \tilde{A}_{(w)}, \tilde{C}_{(w)}, \tilde{R}_{(w)}) \\
 &+ \frac{\sigma^{(-\delta)} h^{(\delta)}}{\Gamma(\delta+1)} E_5(\hat{p}_{(l+1)}, \tilde{S}_{u(l+1)}^P, \tilde{S}_{i(l+1)}^P, \tilde{I}_{(l+1)}^P, \tilde{A}_{(l+1)}^P, \tilde{C}_{(l+1)}^P, \tilde{R}_{(l+1)}^P), \\
 \tilde{R}_{(l+1)} &\approx E_6 + \frac{\sigma^{(-\delta)} h^{(\delta)}}{\Gamma(\delta+2)} \sum_{w=0}^{(l)} \nabla_{w,(l+1)} B_6(\hat{p}_{(w)}, \tilde{S}_{u(w)}, \tilde{S}_{i(w)}, \tilde{I}_{(w)}, \tilde{A}_{(w)}, \tilde{C}_{(w)}, \tilde{R}_{(w)}) \\
 &+ \frac{\sigma^{-\delta} h^{\delta}}{\Gamma(\delta+2)} B_6(\hat{p}_{(l+1)}, \tilde{S}_{u(l+1)}^P, \tilde{S}_{i(l+1)}^P, \tilde{I}_{(l+1)}^P, \tilde{A}_{(l+1)}^P, \tilde{C}_{(l+1)}^P, \tilde{R}_{(l+1)}^P).
 \end{aligned} \tag{50}$$

So, predictor values $\tilde{S}_{u(l+1)}^P, \tilde{S}_{i(l+1)}^P, \tilde{I}_{(l+1)}^P, \tilde{A}_{(l+1)}^P, \tilde{C}_{(l+1)}^P$, and $\tilde{R}_{(l+1)}^P$ are indicated as:

$$\begin{aligned}
 \tilde{S}_{u(l+1)}^P &\approx E_1 + \frac{\sigma^{(-\delta)} h^{(\delta)}}{\Gamma(\delta+1)} \sum_{j=0}^{(l)} \Pi_{j,(l+1)} E_1(\hat{p}_{(w)}, \tilde{S}_{u(w)}, \tilde{S}_{i(w)}, \tilde{I}_{(w)}, \tilde{A}_{(w)}, \tilde{C}_{(w)}, \tilde{R}_{(w)}), \\
 \tilde{I}_{(l+1)}^P &\approx E_3 + \frac{\sigma^{(-\delta)} h^{(\delta)}}{\Gamma(\delta+1)} \sum_{w=0}^{(l)} \Pi_{w,l+1} B_3(\hat{p}_{(w)}, \tilde{S}_{u(w)}, \tilde{S}_{i(w)}, \tilde{I}_{(w)}, \tilde{A}_{(w)}, \tilde{C}_{(w)}, \tilde{R}_{(w)}), \\
 \tilde{A}_{(l+1)}^P &\approx E_4 + \frac{\sigma^{(-\delta)} h^{(\delta)}}{\Gamma(\delta+1)} \sum_{w=0}^{(l)} \Pi_{w,(l+1)} B_4(\hat{p}_{(w)}, \tilde{S}_{u(w)}, \tilde{S}_{i(w)}, \tilde{I}_{(w)}, \tilde{A}_{(w)}, \tilde{C}_{(w)}, \tilde{R}_{(w)}), \\
 \tilde{C}_{(l+1)}^P &\approx E_5 + \frac{\sigma^{(-\delta)} h^{(\delta)}}{\Gamma(\delta+1)} \sum_{w=0}^{(l)} \Pi_{w,(l+1)} B_5(\hat{p}_{(w)}, \tilde{S}_{u(w)}, \tilde{S}_{i(w)}, \tilde{I}_{(w)}, \tilde{A}_{(w)}, \tilde{C}_{(w)}, \tilde{R}_{(w)}), \\
 \tilde{R}_{(l+1)}^P &\approx E_6 + \frac{\sigma^{(-\delta)} h^{(\delta)}}{\Gamma(\delta+1)} \sum_{w=0}^{(l)} \Pi_{w,(l+1)} B_6(\hat{p}_{(w)}, \tilde{S}_{u(w)}, \tilde{S}_{i(w)}, \tilde{I}_{(w)}, \tilde{A}_{(w)}, \tilde{C}_{(w)}, \tilde{R}_{(w)}).
 \end{aligned} \tag{51}$$

where B_1, B_2, B_3, B_4, B_5 and B_6 are given as:

$$\begin{aligned}
B_1(\hat{p}, \tilde{S}_u, \tilde{S}_i, \tilde{I}, \tilde{C}, \tilde{A}, \tilde{R}) &:= X - \frac{\tilde{S}_u \tilde{I} \gamma_1}{\tilde{E}_p} - \tilde{S}_u(\omega_{(1)}^* + \rho_1), \\
B_2(\hat{p}, \tilde{S}_u, \tilde{S}_i, \tilde{I}, \tilde{C}, \tilde{A}, \tilde{R}) &:= \tilde{S}_u \rho_1 - \frac{\tilde{S}_i \tilde{I} \gamma_1}{\tilde{E}_p} (1 - \xi_1) - \tilde{S}_i \omega_{(1)}^*, \\
B_3(\hat{p}, \tilde{S}_u, \tilde{S}_i, \tilde{I}, \tilde{C}, \tilde{A}, \tilde{R}) &:= (\tilde{S}_i(1 - \xi_1) + \tilde{S}_u) \frac{\tilde{I} \gamma_1}{\tilde{E}_p} + \tilde{C} \phi_1 + \tilde{A} \theta_1 - \tilde{I}(\omega_{(1)}^* + \nu_1 + \eta_{(1)}), \\
B_4(\hat{p}, \tilde{S}_u, \tilde{S}_i, \tilde{I}, \tilde{A}, \tilde{C}, \tilde{R}) &:= \tilde{I} \eta_{(1)} - \tilde{A}(\varphi_1 + \omega_{(1)}^* + \theta_1), \\
B_5(\hat{p}, \tilde{S}_u, \tilde{S}_i, \tilde{I}, \tilde{A}, \tilde{C}, \tilde{R}) &:= I \nu_1 - C(\omega_{(1)}^* + \phi_1), \\
B_6(\hat{p}, \tilde{S}_u, \tilde{S}_i, \tilde{I}, \tilde{A}, \tilde{C}, \tilde{R}) &:= \tilde{I} \sigma_1 + \tilde{C} \sigma_2 + \tilde{A} \sigma_3 - \tilde{R} \omega_{(1)}^*.
\end{aligned} \tag{52}$$

Results and discussion

In this section, the graphical representation of the dynamic behavior of an HIV-AIDS model is evaluated. The initial values taken in the simulation are defined as: $E_1 = 129,789,089$, $E_2 = 1 \times 10^8$, $E_3 = 7195$, $E_4 = 3716$, $E_5 = 0$, $E_6 = 0$.

Moreover, the solution behavior of the dynamic model (5) for $\tilde{S}_u, \tilde{S}_i, \tilde{I}, \tilde{A}, \tilde{C}$ and \tilde{R} are simulated via fractional Adaptive-P-C technique against the real data given in Table 2, corresponding varying values of fractional order δ . The following values of the model parameters are considered as $\alpha_1 = 0.3465$, $\alpha_2 = 0.4865$, $\alpha_3 = 0.5465$, $\alpha_4 = 0.6165$ and the initial conditions are $\tilde{S}_u(0) = 129,789,089$, $\tilde{S}_i(0) = 1 \times 10^8$, $\tilde{I}(0) = 7195$, $\tilde{A}(0) = 3716$, $\tilde{C}(0) = 0$ and $\tilde{R}(0) = 0$, and $h = 0.01$.

The numerical results shown in Figs. 2, 3, 4, 5, 6, 7, 8, 9, 10, 11, 12 and 13 indicate the numerical simulation of the model relating to time $T = 50$ years and $E = 675$ for values of $\sigma = 0.9, 1.2$ and various values of $\delta = 0.70, 0.80, 0.90, 1$. The dynamic behavior of different class subpopulations of the model (5) with $\sigma = 0.9$ for distinct values δ are shown in Figs. 2, 3, 4, 5 and 7.

The dynamical behavior of the varying subpopulation classes in the proposed model (5) with $\sigma = 1.2$ for distinct values of δ as shown in Figs. 8, 9, 10, 11, 12 and 13.

A spectrum of subpopulation behavior of the model with $\sigma = 1.2$ for significant measures δ is depicted in the following Fig. 13 below.

Figures 2, 3, 4, 5, 6, 7, 8, 9, 10, 11, 12 and 13 illustrate the graphical depiction of the transmission of the HIV disease model via our considered numerical scheme, along with a comparison between fractional and integer orders. Now, Fig. 2 demonstrates in what manner the number of susceptible uninformed individuals decreases over time, and this decrease is influenced by the fractional order parameter δ . For the small value of δ , the decline in the susceptible uninformed population occurs more gradually. This could imply a slower rate of transition from susceptible to informed or infected states. A gradual decline might suggest that interventions or information dissemination are affecting the uninformed population slowly.

Figure 3 signifies the dynamics of the susceptible informed population. This figure shows that the number of susceptible informed individuals S increases and then stabilizes after a few years. The initial rise in the susceptible informed population could be due to a period of increased information dissemination or initial exposure to preventive measures. This could imply that more individuals are becoming informed and thus moving into this category. After some years, the number of susceptible informed individuals reaches a stable level. This stability might indicate that the population of susceptible informed individuals has reached an equilibrium, where the rate of becoming informed equals the rate of leaving this category. The pattern of growth followed by stabilization suggests that the system is approaching a new steady state after an initial period of change. This could be reflective of a successful information campaign reaching saturation or a balance being struck between new information and other dynamics. Fig. 4 displays that the number of HIV-positive individuals declines as the value of δ decreases. The decline in the HIV-positive population with decreasing fractional order suggests that the dynamics of the HIV-positive population are less aggressive or more stable when the system has less memory or inertia. This could mean that interventions or changes in behavior might have a more gradual or

Parameters	Values	Source	Parameters	Values	Source
X	229,800,000/67.39	³⁴	$\omega_{(1)}^*$	1/67.39	³³
γ_1	0.3465	Fitting	ξ_1	0.3243	Estimated
ρ_1	0.2351	Fitting	$\phi_{(1)}$	0.2059	Fitting
θ_1	0.7661	³⁴	ν_1	3.6523 - e04	Fitting
$\eta_{(1)}$	0.1882	Fitting	φ_1	0.7012	³³
σ_2	$0.2 day^{-1}$	³⁴	\tilde{E}_p	229,800,000	Estimated
σ_1	$0.1 day^{-1}$	³⁴	σ_3	$0.01 day^{-1}$	³⁴

Table 2. Parameters and their values.

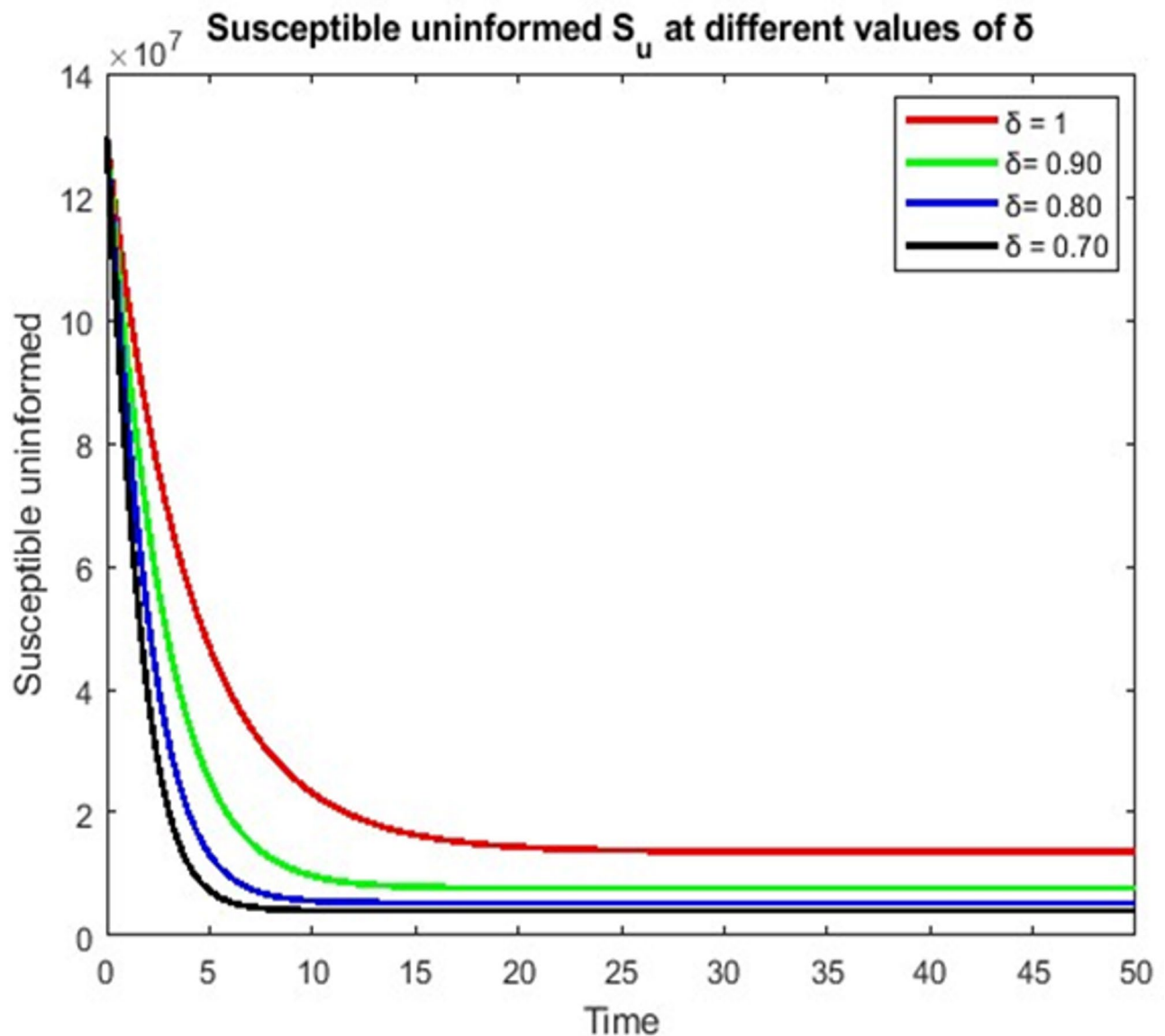


Fig. 2. Dynamical numerical simulation of susceptible uninformed.

less pronounced impact in systems with smaller fractional order parameters. A smaller value of δ might imply a slower or less pronounced response to treatment or intervention, potentially leading to a slower decline in the HIV-positive population compared to a system with a higher fractional order.

As Fig. 5 demonstrates, as the value of the fractional order decreases, correspondingly falls the number of people with AIDS. As lower the fractional order in the proposed model influences the rate of decline of AIDS-afflicted individuals, exactly as it does for the HIV-positive population. In systems with lower values of δ , the dynamics controlling the progression or transition to AIDS may be less aggressive or more stable, as shown by the drop in AIDS-afflicted persons with smaller fractional order.

Figure 6 depicts how the fractional order decreases when the proportion of HIV-positive people taking ART drops. Less memory or inertia in the system is usually represented by a drop in fractional order. In the context of ART, this might suggest that the system's response to ART is slower or less impactful with a lower fractional order. As the system becomes less responsive, the effectiveness or uptake of ART may become less obvious, as seen by the steady throw in the ratio of HIV-positive people getting ART with decreasing fractional order. This may arise from softer dynamics during the transition to treatment or from a slower rate of adaptation to treatment. The finding indicates a system with a smaller fractional order could not see as much continuous growth in the number of people using ART. Improved ART distribution strategies and more responsive medical treatments may be created with an understanding of these dynamics.

Figure 7 demonstrates that the number of recovered persons drops with time. A decreasing number of recovered individuals may indicate that recovery rates are not keeping pace with new infections or that the duration of recovery is limited. This might represent an instance where patients do not remain in a recovered

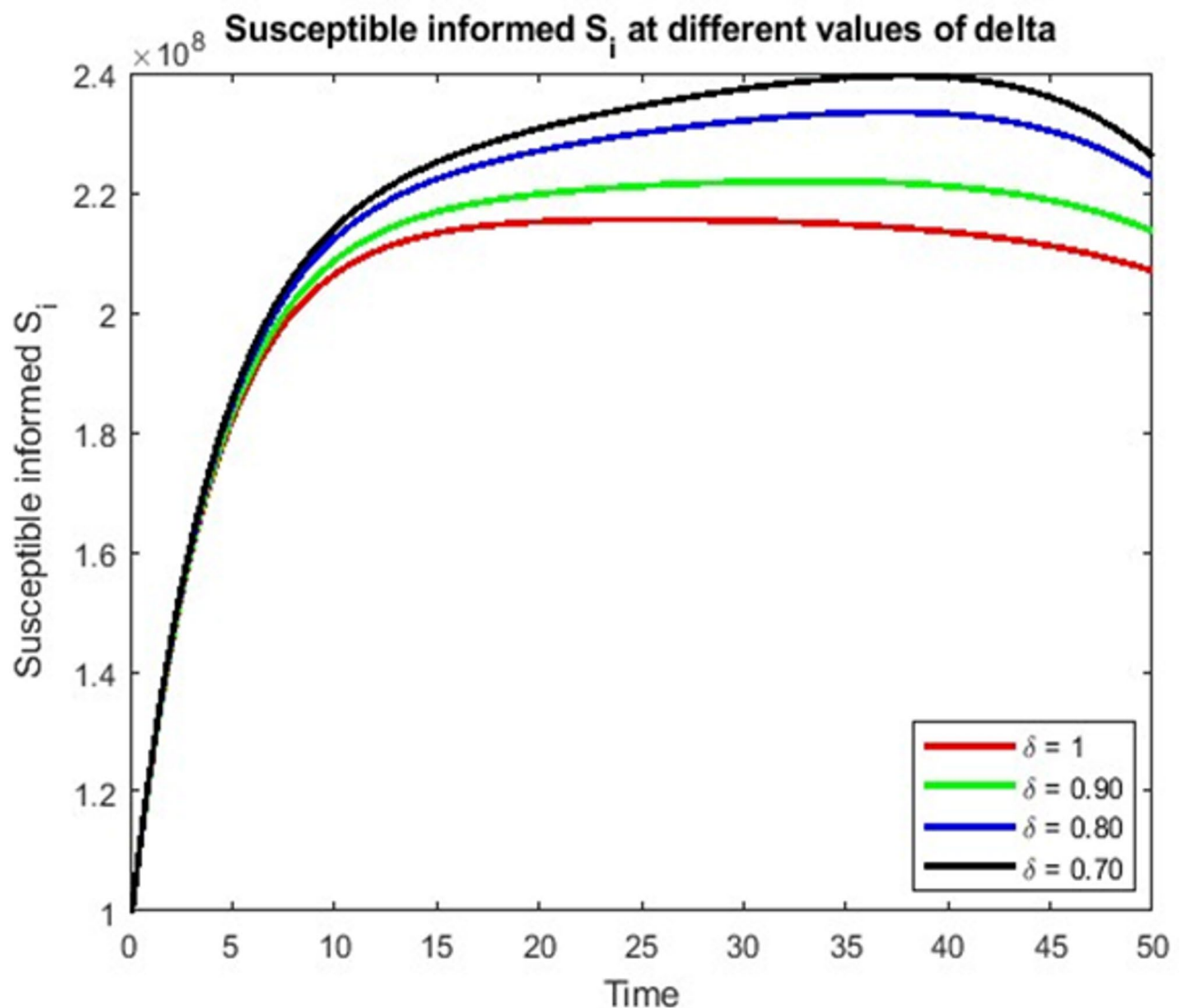


Fig. 3. Dynamical numerical simulation of susceptible informed.

condition for long or if recovery rates are inadequate relative to the number of new cases. If the model incorporates fractional order, this decline might be influenced by the δ . For instance, a lower value of δ might mean slower or less pronounced recovery dynamics, leading to a slower accumulation of recovered individuals. This result highlights the need for continuous and effective interventions to ensure that more individuals transition to a recovered state. If the decline is significant, it may indicate the need for revisiting treatment or intervention strategies to improve recovery rates and ensure sustainable health outcomes.

Similarly, when with $\sigma = 1.2$ Fig. 8 shows the susceptible uninformed populace increased slowly with a smaller fractional order. According to Fig. 9, the number of susceptible informed populace increases for the different fractional order. Figure 10 shows the populace with HIV infected gradually increasing over time. Figure 11 displays the number of AIDS-afflicted people increased with a smaller fractional order. Figure 12 illustrates that the populace receiving ART gradually increased over time and it indicates the great impact on society. Figure 13 shows that the recovered individual increased with a smaller fractional order. The numerical simulation, shown in Figs. 8, 9, 10, 11, 12 and 13, demonstrates that early detection and treatment are effective in eradicating the disease. Public awareness about HIV-AIDS prevention has increased, and the use of contraception and microbicides has been explored as additional control measures. As a result, more people are aware of the disease, and receiving ART, and the number of AIDS patients recovering has increased. The study could be further expanded by considering a hypothetical vaccine and the reduction of intimate activities by some individuals with AIDS. It was observed that varying the value of δ leads to different trajectories, and the graphs indicate that the system's dynamic behavior is modified by a fractional derivative of order two. Understanding these dynamics through the figures provides valuable insights into how mathematical models can inform public health strategies and improve the management of HIV/AIDS.

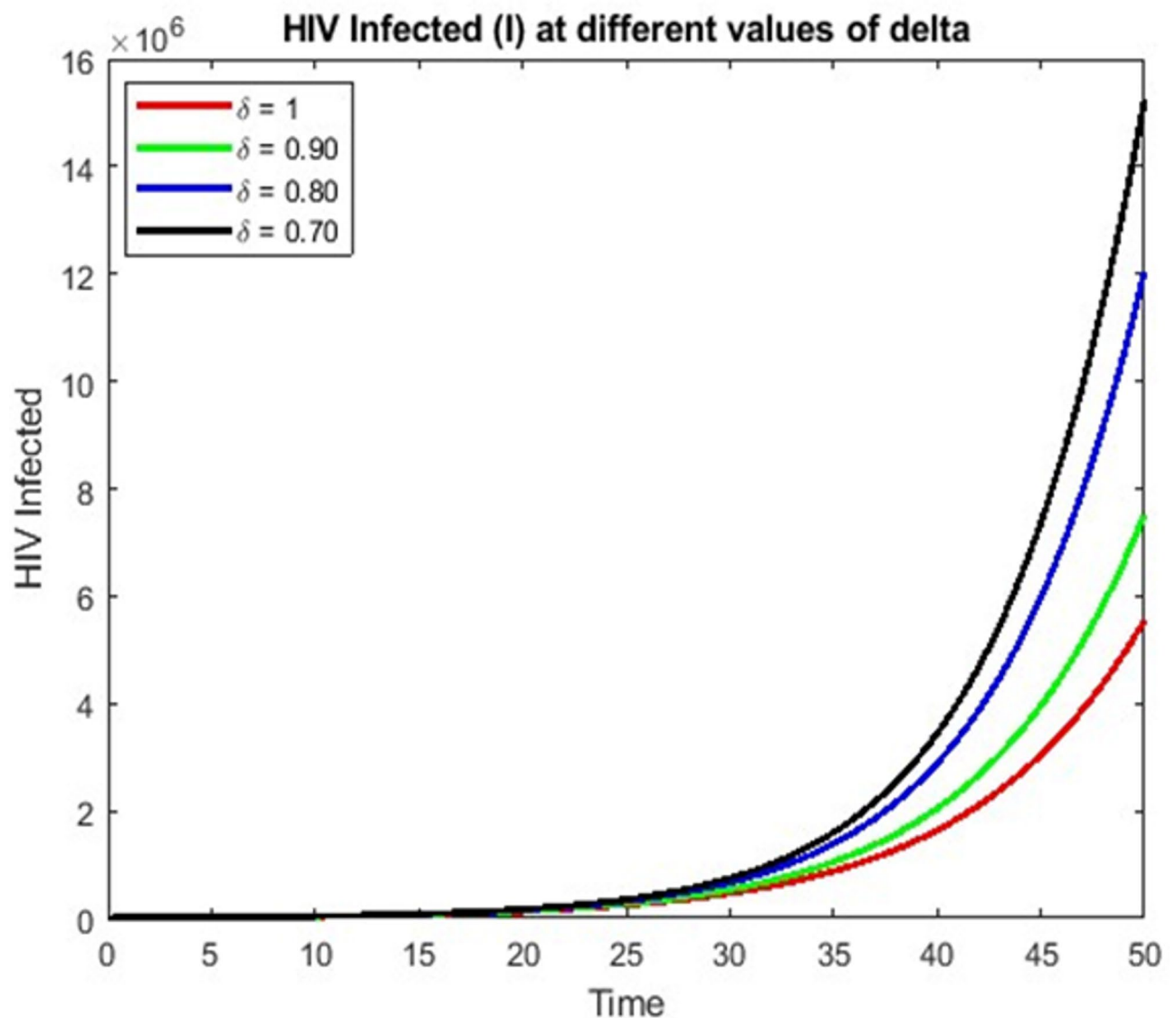


Fig. 4. Dynamical simulation of HIV infected.

Conclusion

Mathematical modeling plays an important role in understanding and handling infectious diseases such as HIV. Comparing nonlinear compartmental models to traditional models, the first offers a more sophisticated understanding of disease transmission. In order to investigate numerical insights into the transmission dynamics of the HIV disease, a fractional order model by incorporating antiretroviral treatment (ART) is introduced. The rate at which the infected population getting ART transitions to recovered persons (R) and the frequency of hospitalized patients' recovery progress are specifically measured via the devised model. We applied the fractional derivative operators to capture more natural phenomena of the proposed model. A more realistic and exact understanding of how procedures impact different populations and how recovery dynamics change over time is also made possible by this model.

Throughout the investigation, a comprehensive analysis is conducted, covering key aspects such as positivity, boundedness, equilibrium points, the basic reproduction number, stability, and sensitivity. The model ensures boundedness and positivity by incorporating constraints and selecting appropriate functional forms, preventing unrealistic variable growth, and aligning the model with real-world constraints. This precautionary approach enhances the model's reliability and applicability, providing policymakers with an accurate representation that supports well-informed decision-making within practical limitations.

The analysis of stability in the model indicates that when $R_0 < 1$, the system is both locally and globally asymptotically stable at the disease-free equilibrium D_0 . Conversely, if $R_0 > 1$, the system exhibits an endemic equilibrium D^* , at which point it is locally and globally asymptotically stable. Furthermore, a sensitivity analysis is conducted to assess the impact of various compartmental parameters on the basic reproduction number. The existence and uniqueness of the fractional-order model are established using the framework of fixed-point theory.

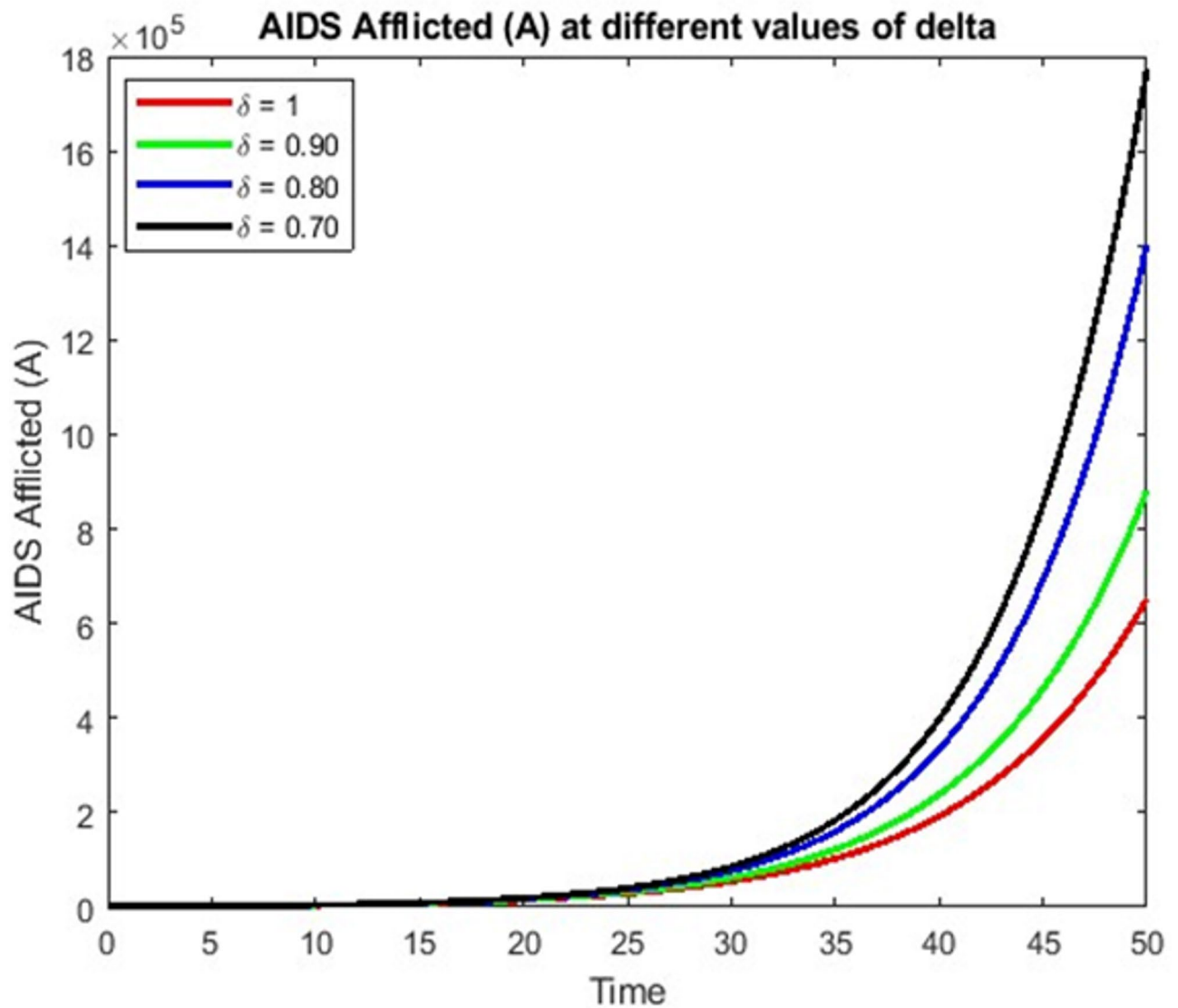


Fig. 5. Dynamical simulation of AIDS afflicted.

To solve the nonlinear differential equations, a modified fractional Caputo operator is employed alongside an adaptive predictor-corrector approach. A quantitative study is performed to compare the effects of integer-order and fractional-order models, and numerical results are obtained using the adaptive predictor-corrector strategy. The graphical results demonstrated that the outcomes are significantly influenced by the fractional order parameters σ and δ . Numerical simulations at different fractional orders, along with a comparative analysis against integer-order models, further illustrate the model's predictive capability. The numerical implementation using a predictor-corrector scheme in MATLAB enhances computational efficiency, improving the validation of theoretical findings. The results suggest that both susceptible informed and susceptible ignorant individuals significantly impact the number of infected individuals. The overall infection rate exhibits smoother transitions and prolonged peaks in the infected population due to the interplay between fractional-order dynamics in susceptible and ignorant individuals. Additionally, individuals who recover from the virus or transition through antiretroviral therapy (ART) are classified as recovered. The process of recovery is influenced by infection rates and interactions between compartments which leads to a more gradual increase in the recovered population and potentially longer periods of recovery dynamics. Moreover, the extended compartment $R(t)$ demonstrates that the infected population under ART progresses toward recovery, reinforcing the importance of treatment interventions in managing disease spread.

This model offers a more precise and realistic depiction of disease transmission, the impact of interventions on different populations, and the evolution of recovery dynamics over time. The existing analysis can be extended by integrating various fractional operators that integrate non-local and non-singular kernels, enhancing the mathematical modeling of HIV/AIDS and improving future predictions and intervention strategies. Moreover, future directions for a temporal fractional HIV/AIDS model with fractal dimensions comprise refining parameter estimation, incorporating socioeconomic factors, and leveraging machine learning to enhance forecasting

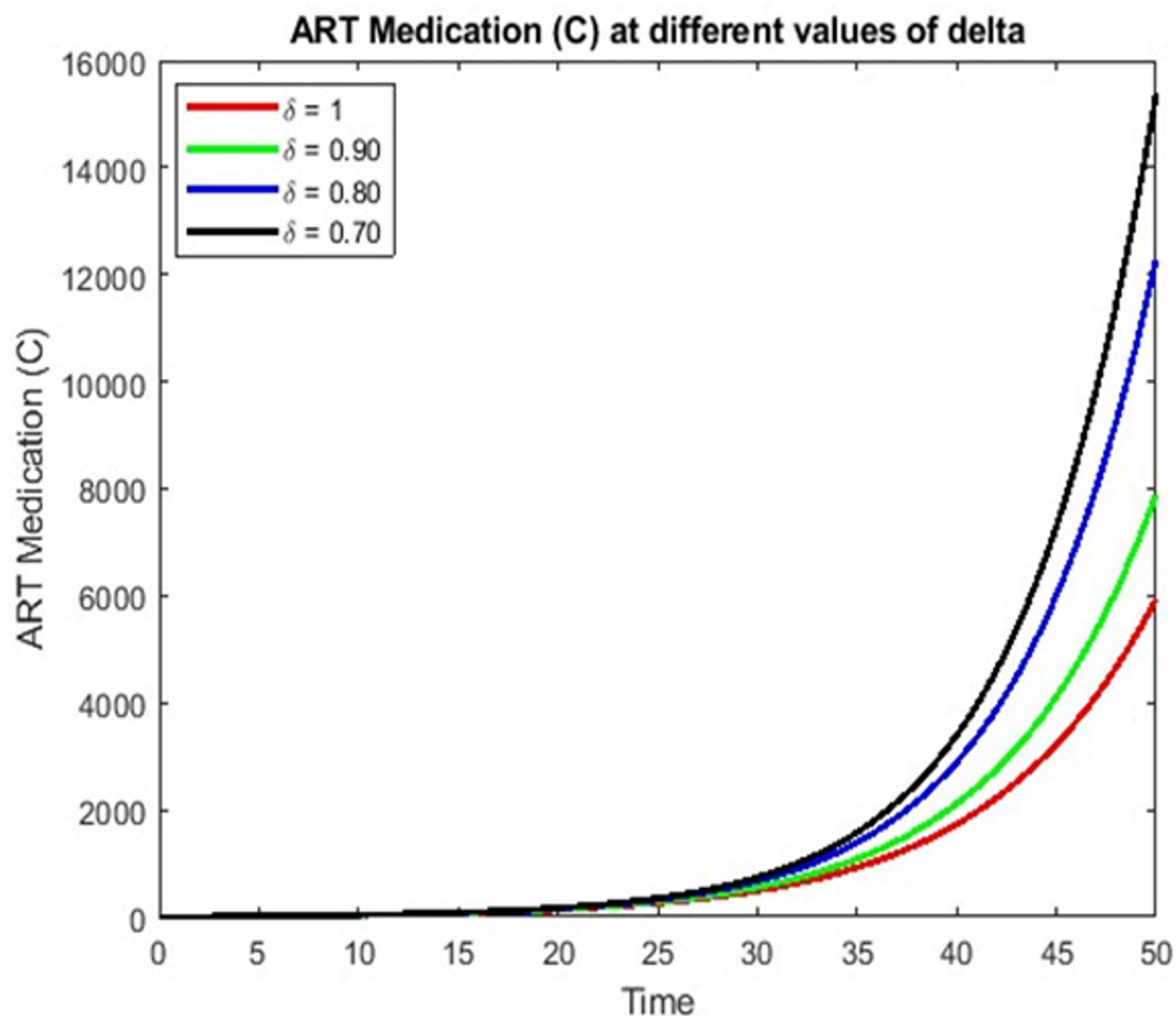


Fig. 6. Dynamical simulation of ART medication.

accuracy. Expanding the model to multiple locations, enabling real-time monitoring, and exploring different intervention scenarios can further increase its effectiveness. The model's adaptability allows for customization based on regional needs, and its implementation in public health education can contribute to raising awareness. This research advances the field of fractional epidemiology, paving the way for similar methodologies to be applied in studying other infectious diseases.

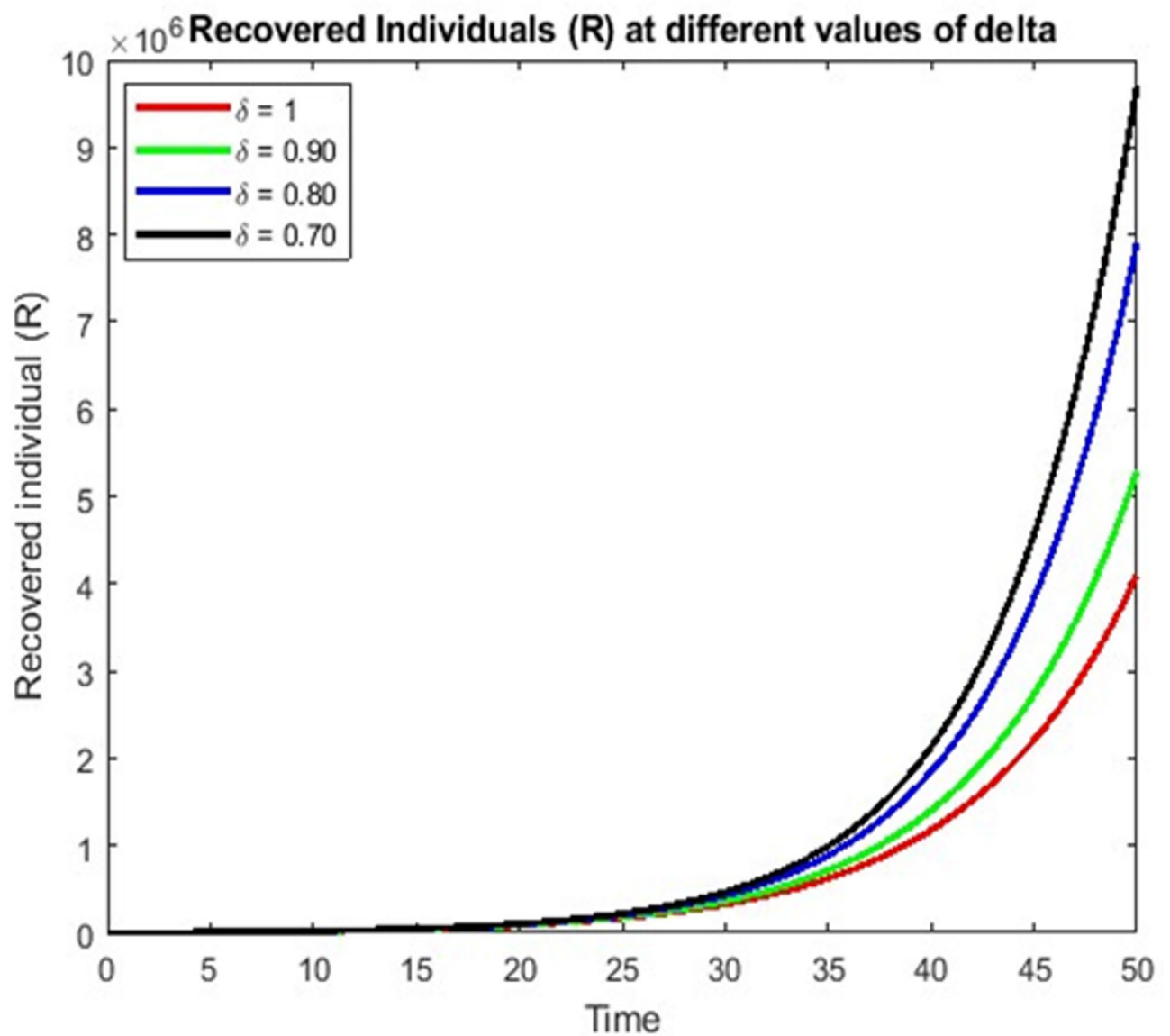


Fig. 7. Dynamical simulation of recovered individuals.

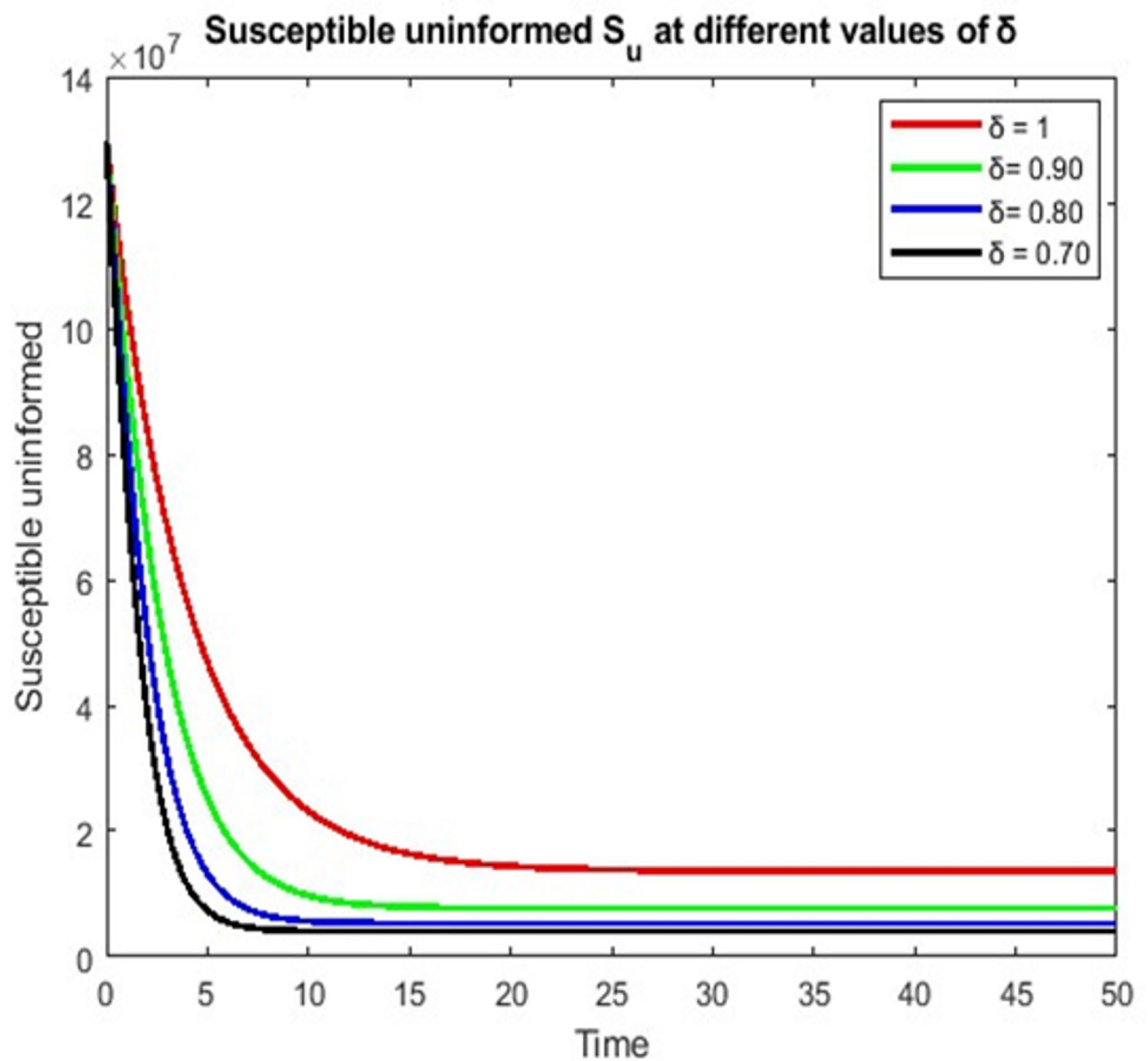


Fig. 8. Dynamical simulation of susceptible uninfected.

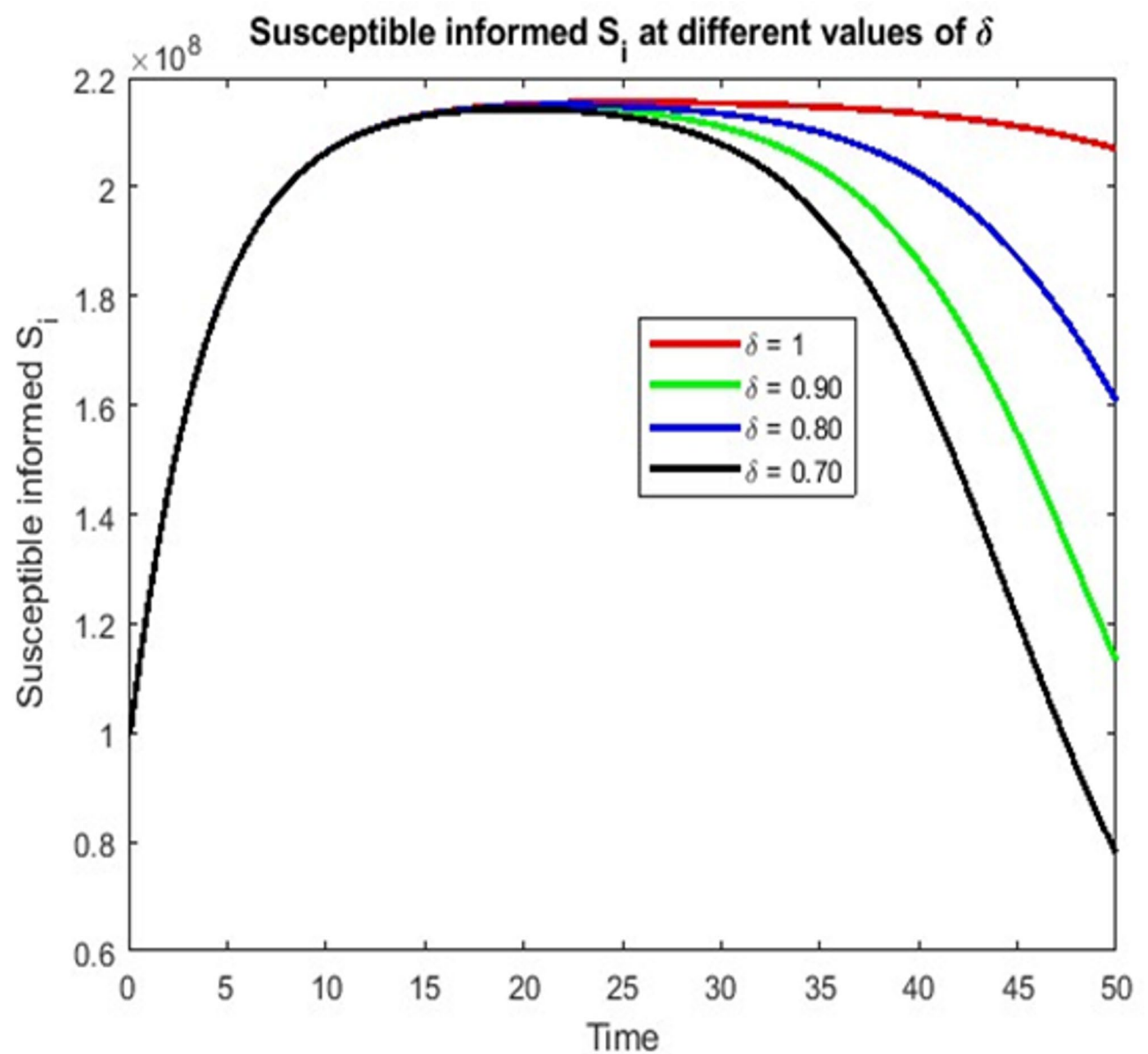


Fig. 9. Dynamical simulation of susceptible informed.

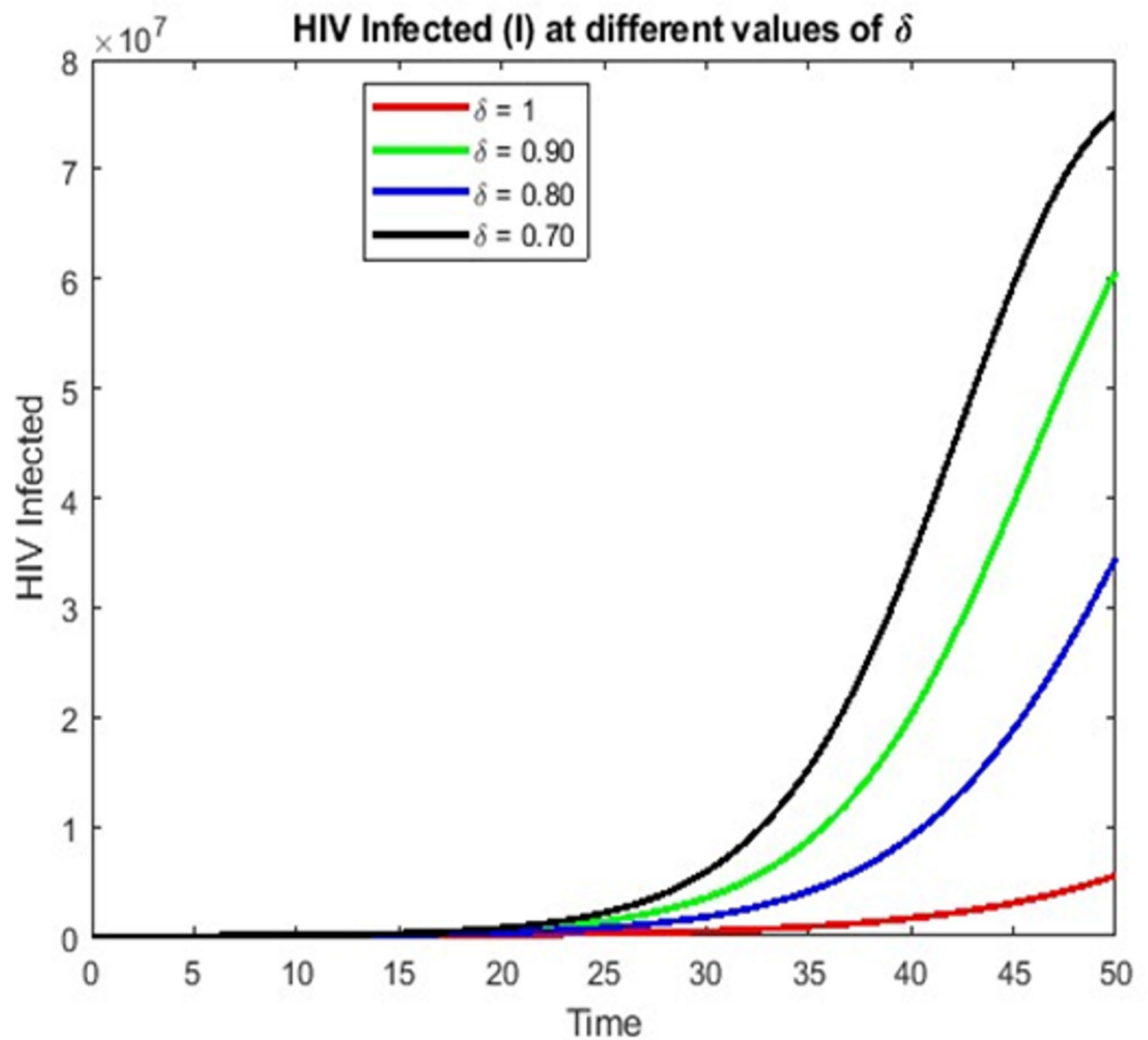


Fig. 10. Dynamical simulation of HIV infected.

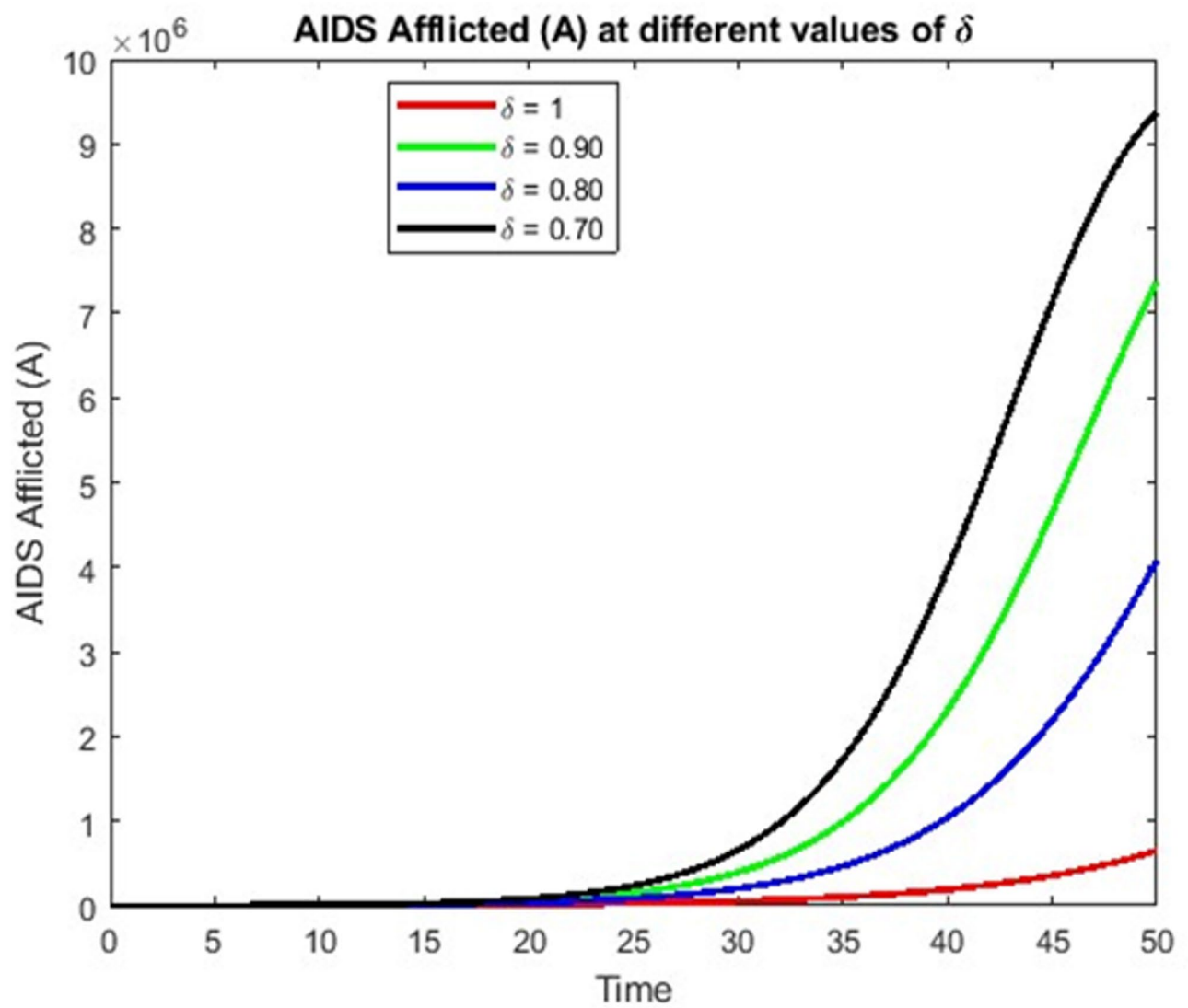


Fig. 11. Dynamical simulation of AIDS afflicted.

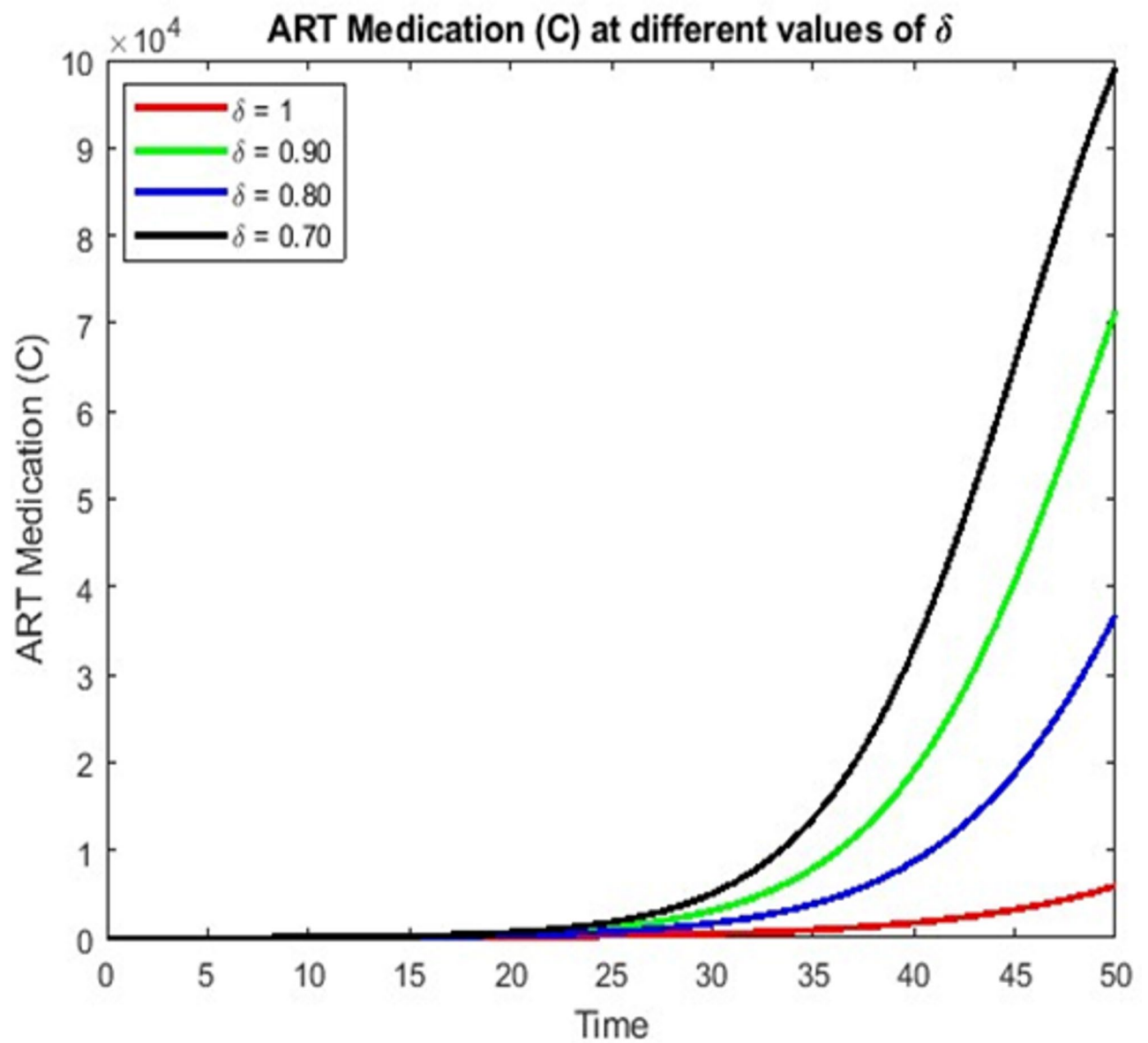


Fig. 12. Dynamical simulation of ART medication.

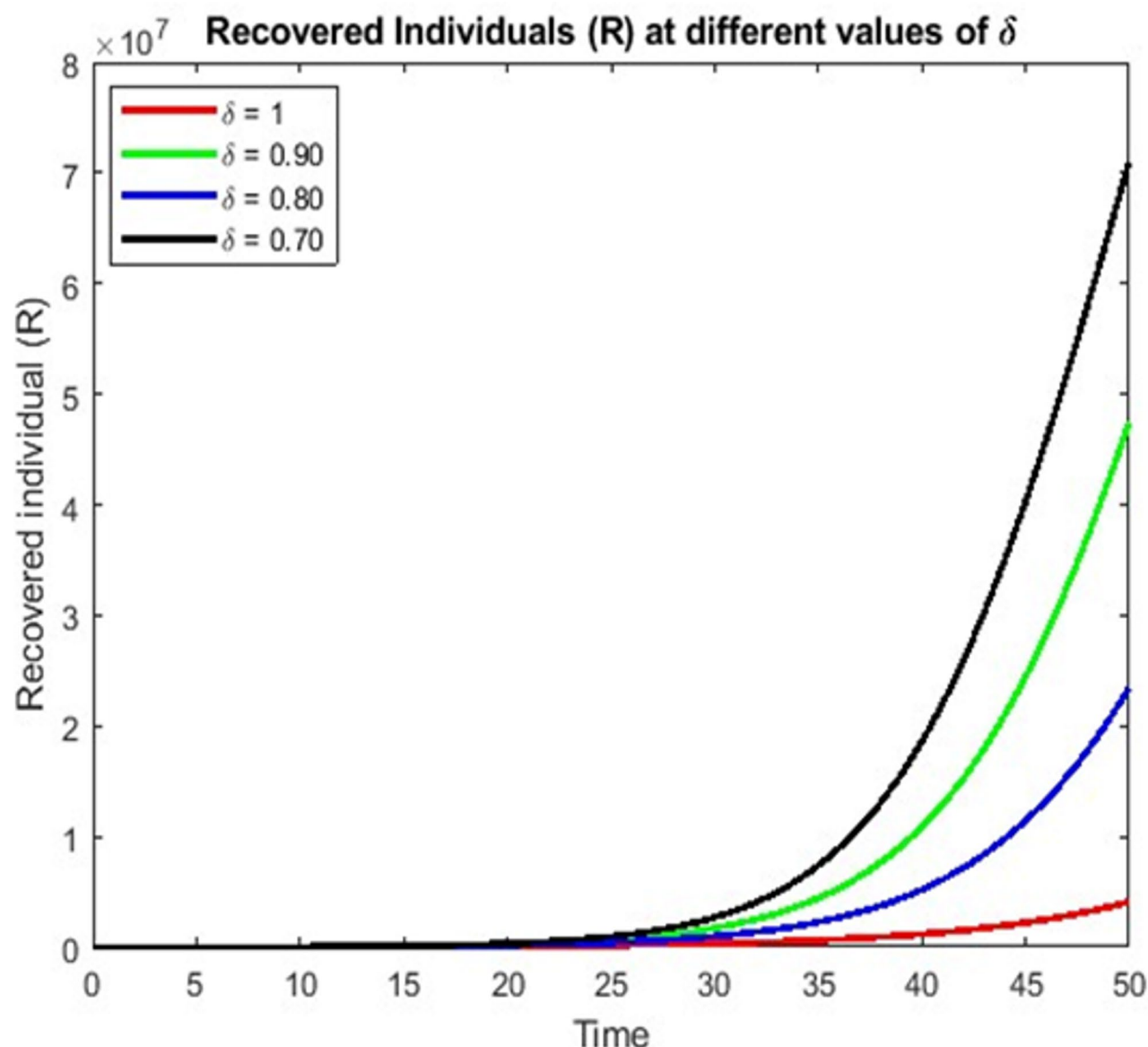


Fig. 13. Dynamical simulation of recovered individual.

Data availability

The datasets used and/or analysed during the current study available from the corresponding author on reasonable request.

Received: 11 February 2025; Accepted: 6 May 2025

Published online: 25 May 2025

References

1. World Health Organization. HIV <https://www.who.int/gho/hiv/en>
2. Swinkels, H., Vaillant, A. J., Nguyen, A. & Gulick, P. HIV and AIDS. *StatPearls* (2024).
3. Deeks, S. G., Lewin, S. R. & Havlir, D. V. The end of AIDS: HIV infection as a chronic disease. *Lancet*. **382** (9903), 1525–1533 (2013).
4. Baleanu, D., Hasanabadi, M., Vaziri, A. M. & Jajarmi, A. A new intervention strategy for an HIV/AIDS transmission by a general fractional modeling and an optimal control approach. *Chaos Solitons Fractals*. **167**, Article ID: 113078 (2023).
5. Gao, W., Veerasha, P., Baskonus, H. M., Prakasha, D. G. & Kumar, P. A new study of unreported cases of 2019-nCoV epidemic outbreaks. *Chaos Solitons Fractals*. **138**, 109929 (2020).
6. Atangana, A. & Owolabi, K. M. New numerical approach for fractional differential equations. *Math. Model. Nat. Phenom.* **13** (1), 3 (2018).
7. Gao, W., Veerasha, P., Baskonus, H. M., Prakasha, D. G. & Kumar, P. A new study of unreported cases of 2019-nCoV epidemic outbreaks. *Chaos Solitons Fractals*. **138**, 1–6 (2020).

8. Baleanu, D., Wu, G. C. & Zeng, S. D. Chaos analysis and asymptotic stability of generalized Caputo fractional differential equations. *Chaos Solitons Fractals*. **102**, 99–105 (2017).
9. Fall, A. N., Ndiaye, S. N. & Sene, N. Black–Scholes option pricing equations described by the Caputo generalized fractional derivative. *Chaos Solitons Fractals*. **125**, 108–118 (2019).
10. Ayele, T. K., Goufo, E. F. D. & Mugisha, S. Mathematical modeling of HIV/AIDS with optimal control: a case study. *Ethiopia Results Phys.* **26**, 1–17 (2021).
11. Li, S. et al. M., The impact of standard and nonstandard finite difference schemes on HIV nonlinear dynamical model. *Chaos Solitons Fractals*. **173**, Article ID 113755 (2023).
12. Roy, P. K., Chatterjee, A. N., Greenhalgh, D. & Khan, Q. J. Long term dynamics in a mathematical model of HIV-1 infection with delay in different variants of the basic drug therapy model. *Nonlinear Anal. Real. World Appl.* **14** (3), 1621–1633 (2013).
13. Cai, L., Li, X., Ghosh, M. & Guo, B. Stability analysis of an HIV/AIDS epidemic model with treatment. *J. Comput. Appl. Math.* **229** (1), 313–323 (2009).
14. Goyal, M., Baskonus, H. M. & Prakash, A. Regarding new positive, bounded and convergent numerical solution of nonlinear time fractional HIV/AIDS transmission model. *Chaos Solitons Fractals*. **139** Article ID: 110096 (2020).
15. Aslam, M. et al. A fractional order HIV/AIDS epidemic model with Mittag-Leffler kernel. *Adv. Differ. Equ.* **2021**, 1–15 (2021).
16. Iqbal, Z. et al. Positivity and boundedness preserving numerical algorithm for the solution of fractional nonlinear epidemic model of HIV/AIDS transmission. *Chaos Solitons Fractals*. **134**, Article ID: 109706 (2020).
17. Shaiful, E. M. & Utoyo, M. I. A fractional-order model for HIV dynamics in a two-sex population. *Int. J. Math. Math. Sci.* **2018**, 1–12 (2018).
18. Jan, R., Khan, A., Boulaaras, S. & Ahmed Zubair, S. Dynamical behaviour and chaotic phenomena of HIV infection through fractional calculus. *Discrete Dyn. Nat. Soc.* **2022** (2022).
19. Naik, P. A., Zu, J. & Owolabi, K. M. Modeling the mechanics of viral kinetics under immune control during primary infection of HIV-1 with treatment in fractional order. *Phys. A Stat. Mech. Appl.* **545**, Article ID: 123816 (2020).
20. Piqueira, J. R. C., Castaño, M. C. & Monteiro, L. H. A. Modeling the spreading of HIV in homosexual populations with heterogeneous preventive attitude. *J. Biol. Syst.* **12** (04), 439–456 (2004).
21. Kumar, S., Chauhan, R. P., Osman, M. S. & Mohiuddine, S. A. A study on fractional HIV-AIDS transmission model with awareness effect. *Math. Methods Appl. Sci.* **46** (7), 8334–8348 (2023).
22. Katugampola, U. N. New approach to a generalized fractional integral. *Appl. Math. Comput.* **218** (3), 860–865 (2011).
23. Jarad, F., Abdeljawad, T. & Baleanu, D. On the generalized fractional derivatives and their Caputo modification. *J. Nonlinear Sci. Appl.* **10** (5), 2607–2619 (2017).
24. Katugampola, U. N. A new approach to generalized fractional derivatives. *arXiv preprint arXiv:1106.0965*. (2011).
25. Diethelm, K., Ford, N. J. & Freed, A. D. A predictor-corrector approach for the numerical solution of fractional differential equations. *Nonlinear Dyn.* **29**, 3–22 (2002).
26. Anjam, Y. N., Alqahtani, R. T., Alharthi, N. H. & Tabassum, S. Unveiling the complexity of HIV transmission: integrating Multi-Level infections via Fractal-Fractional analysis. *Fractal Fract.* **8** (299), 1–21 (2024).
27. Liu, X., Ahmad, S., Rahman, M. U., Nadeem, Y. & Akgül, A. Analysis of a TB and HIV co-infection model under Mittag-Leffler fractal-fractional derivative. *Phys. Scr.* **97** (5), 054011 (2022).
28. Anjam, Y. N. et al. A fractional order investigation of smoking model using Caputo-Fabrizio differential operator. *Fractal Fract.* **6**, 623 (2022).
29. Anjam, Y. N., Shahid, I., Emadifar, H., Cheema, S. A. & Rahman, M. U. Dynamics of the optimality control of transmission of infectious disease: a sensitivity analysis. *Sci. Rep.* **14** (1), 1041 (2024).
30. Verma, L., Meher, R. & Pandya, D. P. Parameter estimation study of temporal fractional HIV/AIDS transmission model with fractal dimensions using real data in India. *Math. Comput. Simul.* (2025).
31. Khan, M. A. & Odinsyah, H. P. Fractional model of HIV transmission with awareness effect. *Chaos Solitons Fractals*. **138**, 109967 (2020).
32. Kumar, P., SM, S. & Govindaraj, V. Forecasting of HIV/AIDS in South Africa using 1990 to 2021 data: novel integer-and fractional-order fittings. *Int. J. Dyn. Control.* **12** (7), 2247–2263 (2024).
33. Meetei, M. Z. et al. A Analysis and simulation study of the HIV/AIDS model using the real cases. *PLoS One*. **19**(6), e0304735 (2024).
34. Guedri, K. et al. A numerical study of HIV/AIDS transmission dynamics and the onset of long-term disability in chronic infection. *Eur. Phys. J. Plus.* **139** (12), 1–24 (2024).
35. Zarin, R., Khan, A. & Kumar, P. Fractional-order dynamics of Chagas-HIV epidemic model with different fractional operators. *AIMS Math.* **7** (10), 18897–18924 (2022).
36. Chu, Y. M., Zarin, R., Khan, A. & Murtaza, S. A vigorous study of fractional order mathematical model for SARS-CoV-2 epidemic with Mittag-Leffler kernel. *Alex. Eng. J.* **71**, 565–579 (2023).
37. Zarin, R. A robust study of dual variants of SARS-CoV-2 using a reaction-diffusion mathematical model with real data from the USA. *Eur. Phys. J. Plus.* **138** (11), 1–23 (2023).
38. Guedri, K., Zarin, R., Oreijah, M., Alharbi, S. K. & Khalifa, H. A. E. W. Artificial neural network-driven modeling of Ebola transmission dynamics with delays and disability outcomes. *Comput. Biol. Chem.* **115**, 108350 (2025).
39. Okongo, W., Okelo Abonyo, J., Kioi, D., Moore, S. E., Aguegbah, N. & S. Mathematical modeling and optimal control analysis of Monkeypox virus in contaminated environment. *Model. Earth Syst. Environ.* **10** (3), 3969–3994 (2024).
40. Aguegbah, N. S., Phineas, K. R., Felix, M. & Diallo, B. Modeling and control of hepatitis B virus transmission dynamics using fractional order differential equations. *Commun. Math. Biol. Neurosci.* **2023**, 107 (2023).
41. Aguegbah, N. S. et al. A novel approach to modeling malaria with treatment and vaccination as control strategies in Africa using the Atangana–Baleanu derivative. *Model. Earth Syst. Environ.* **11** (2), 110 (2025).
42. Diallo, B. et al. Fractional optimal control problem modeling bovine tuberculosis and rabies co-infection. *Results Control Optim.* **18**, 100523 (2025).

Author contributions

L.H.: My contribution to this article is to develop the main idea of research. A.A.: My contribution to this article is to develop the objectives, identify the research gap, and outline the methodology. Y.N.A.: My contribution to this article involved writing and reviewing the manuscript. B.R.: My contribution to this manuscript was verifying and reviewing the results. M.A.T.: I contributed to the Analysis section and edited certain parts of manuscript.

Funding

Research for this article was funded by Chongqing Key Discipline "Infectious Disease Prevention and Control Project".

Declarations

Competing interests

The authors declare no competing interests.

Additional information

Correspondence and requests for materials should be addressed to A.A.

Reprints and permissions information is available at www.nature.com/reprints.

Publisher's note Springer Nature remains neutral with regard to jurisdictional claims in published maps and institutional affiliations.

Open Access This article is licensed under a Creative Commons Attribution-NonCommercial-NoDerivatives 4.0 International License, which permits any non-commercial use, sharing, distribution and reproduction in any medium or format, as long as you give appropriate credit to the original author(s) and the source, provide a link to the Creative Commons licence, and indicate if you modified the licensed material. You do not have permission under this licence to share adapted material derived from this article or parts of it. The images or other third party material in this article are included in the article's Creative Commons licence, unless indicated otherwise in a credit line to the material. If material is not included in the article's Creative Commons licence and your intended use is not permitted by statutory regulation or exceeds the permitted use, you will need to obtain permission directly from the copyright holder. To view a copy of this licence, visit <http://creativecommons.org/licenses/by-nc-nd/4.0/>.

© The Author(s) 2025